

Attachment 4

NET-264-02 P, Revision 3, "Criticality Analysis of the Peach Bottom Spent Fuel Racks for GNF 2 Fuel with Boraflex Panel Degradation Projected to May 2010" (Non-Proprietary Version)

Criticality Analysis of the Peach Bottom Spent Fuel Racks for GNF 2 Fuel with Boraflex Panel Degradation Projected to May 2010

Prepared

for

Exelon Nuclear
Under Purchase Order: 01003029

by:

Northeast Technology Corp.
108 North Front Street
UPO Box 4178
Kingston, New York 12402

Revision:	Date:	Prepared by:	Reviewed By:	Approved By: (QA)
2	3/6/09	Matthew C. Harris	[Signature]	L.P. Mariani
3	5/15/09	Matthew C. Harris	[Signature]	L.P. Mariani

Note: New revision signature sheet initiated due to the fact that Revision 2 of NET-264-02 included a change of title.

Table of Contents

1.0	Introduction.....	1
2.0	Peach Bottom Unit 2 Spent Fuel Racks	3
2.1	Spent Fuel Rack Description	3
3.0	RACKLIFE Projections	6
3.1	Model Overview and Assumptions.....	6
3.2	Projections through 2010.....	7
4.0	The Reactivity Effects of Boraflex Degradation	15
4.1	Introduction	15
4.1.1	Uniform Dissolution	15
4.1.2	Shrinkage, Including Gaps	15
4.1.3	Local Dissolution	16
4.2	Methodology for Projecting Future Panel Conditions	16
4.3	Methodology for Assessing the Reactivity Effects of Boraflex Degradation	20
4.4	Results.....	22
5.0	Results of the Criticality Analysis.....	27
5.1	Design Basis and Design Criteria	27
5.2	Analytical Methods and Assumptions	28
5.3	Calculated Results	31
5.3.1	Reference Eigenvalue Calculations	31
5.3.2	CASMO-4 and KENO V.a Reactivity Calculations in Core and in Rack Geometries	35
5.3.3	Effect of Tolerances and Uncertainties	36
5.3.4	Space Between Modules	39
5.3.5	Summary of Reactivity Calculations.....	39
5.3.6	Abnormal/Accident Conditions	39
6.0	Conclusions	42

List of Figures

Figure 2-2:	Peach Bottom Storage Cell Elements.....	5
Figure 3-1:	Occupied Cells in the Peach Bottom 2 Spent Fuel Storage Racks on February 26, 2006.	9
Figure 3-2:	Projected Occupied Cells in the Peach Bottom 2 Spent Fuel Storage Racks on May 1, 2010.	10
Figure 3-3:	Predicted Boron Carbide Loss through February 26, 2006 in the Peach Bottom Spent Fuel Storage Racks.....	11
Figure 3-4:	Panel Absorbed Dose through February 26, 2006 in the Peach Bottom Spent Fuel Storage Racks	12
Figure 3-5:	Predicted Boron Carbide Loss through May 1, 2010 in the Peach Bottom Spent Fuel Storage Racks	13
Figure 3-6:	Panel Absorbed Dose through May 1, 2010 in the Peach Bottom Spent Fuel Storage Racks	14
Figure 4-1:	Typical Model of an Peach Bottom Unit 2 Boraflex Panel.....	25
Figure 4-2:	Sample Distribution of Panel Degradation Reactivity Effects.....	26
Figure 5-1:	Rack Reactivity versus Burnup for the GNF 2 Fuel Type in the Peach Bottom Unit 2 Spent Fuel Storage Racks.	34

List of Tables

Table 4-1:	Conservative Reactivity Effects of Cracks Undetected by BADGER	23
Table 4-2:	Reactivity Effects of Uniform Boraflex Panel Thinning	23
Table 4-3:	Reactivity Effects of Degraded Panels	24
Table 5-1	GNF 2 Fuel Assembly Description Peach Bottom Nuclear Generating Station.....	33
Table 5-2	CASMO-4/KENO V.a Reactivity Comparison in Core Geometry: GNF 2 Bundles @ [] w/o U-235 ([]% T.D.), Zero Burnup.....	35
Table 5-3	CASMO-4/KENO V.a Reactivity Comparison in Rack Geometry: GNF 2 Bundles @ [] w/o U-235 ([]% T.D.), Zero Burnup.....	35

1.0 Introduction

The Peach Bottom Unit 2 spent fuel pool was refitted with high density spent fuel storage racks in 1986. These racks were fabricated by the Westinghouse Corporation and utilize the neutron absorber material Boraflex for reactivity control^[1,2]. Boraflex has been observed to be subject to in-service degradation from the combined effects of gamma radiation from spent fuel and long term exposure to the aqueous pool environment.

To assure acceptable in service Boraflex performance Exelon Nuclear has initiated a multi-prong surveillance program. This program includes monitoring pool reactive silica levels, BADGER testing^[3] and tracking the current and projected performance of each panel of Boraflex in the Peach Bottom pools with RACKLIFE^[4,5]. To date three BADGER test campaigns have been completed in the Unit 2 SFP (1996^[6], 2002^[7] and 2006^[8]) and two campaigns have been completed in the Unit 3 SFP (2001^[9] and 2005^[10]). The Peach Bottom Unit 2 RACKLIFE model has been verified by the three BADGER campaigns that also show the Unit 2 spent fuel racks are bounding with respect to Boraflex degradation. This model has been used to predict the in-service degradation of each Boraflex panel through May 1, 2010. | 2

This report documents the application of an advanced methodology developed by Northeast Technology Corp. for assessing the safe storage of GNF 2 fuel in the Westinghouse spend fuel racks with degraded Boraflex^[11]. This assessment is made through May 2010 and utilized the results of the most recent Unit 2 BADGER test data sets to establish distributions of local and global panel degradation at the time of the testing. The RACKLIFE results are then used to track the progression of average panel degradation and project the condition of the Boraflex in May 2010. A special algorithm, developed by NETCO, is then applied to the BADGER data to project the local and global panel degradation based on the RACKLIFE prediction of panel average boron carbide loss. | 2

2.0 Peach Bottom Unit 2 Spent Fuel Racks

2.1 Spent Fuel Rack Description

The spent fuel racks at Peach Bottom are shown in Figure 2-1. The racks consist of 15 modules of varying size for a total capacity of 3814 storage cells. These racks utilize Boraflex as a poison and contain the panels that were selected for BADGER testing^[8].

In the design of the racks, one sheet of Boraflex is positioned between opposing faces of the fuel assemblies. The individual storage cells are formed by creating a checkerboard configuration of square tubes as shown in Figure 2-2. The basic structure of this storage array is a square stainless steel tube [] inches thick with a [] inch inside dimension and 169 inches in length. Each structural tube has one sheet of Boraflex [] inches long, [] inches wide, and [] inches thick (nominal) positioned on each of the four outside faces. During manufacture, the Boraflex sheets were first attached to [] inches thick stainless steel wrapper plates using a Dow silicone sealant that served as an adhesive. The wrapper plates were then tack welded to the structural cell wall. Tack welds are located on approximately []-inch centers along the length of the wrapper plate.

To complete the rack module assembly, the structural tubes with Boraflex and stainless steel cover plates are welded together at the corners and to a bottom base plate. In this manner, every other storage location is formed by the structural tube and the resultant locations are formed by the four adjacent faces of neighboring structural tubes. The base plates of each module are fitted with leveling feet that rest on the pool floor.

NET-264-02 NP
Non-Proprietary Information Submitted in
Accordance with 10 CFR 2.390



North

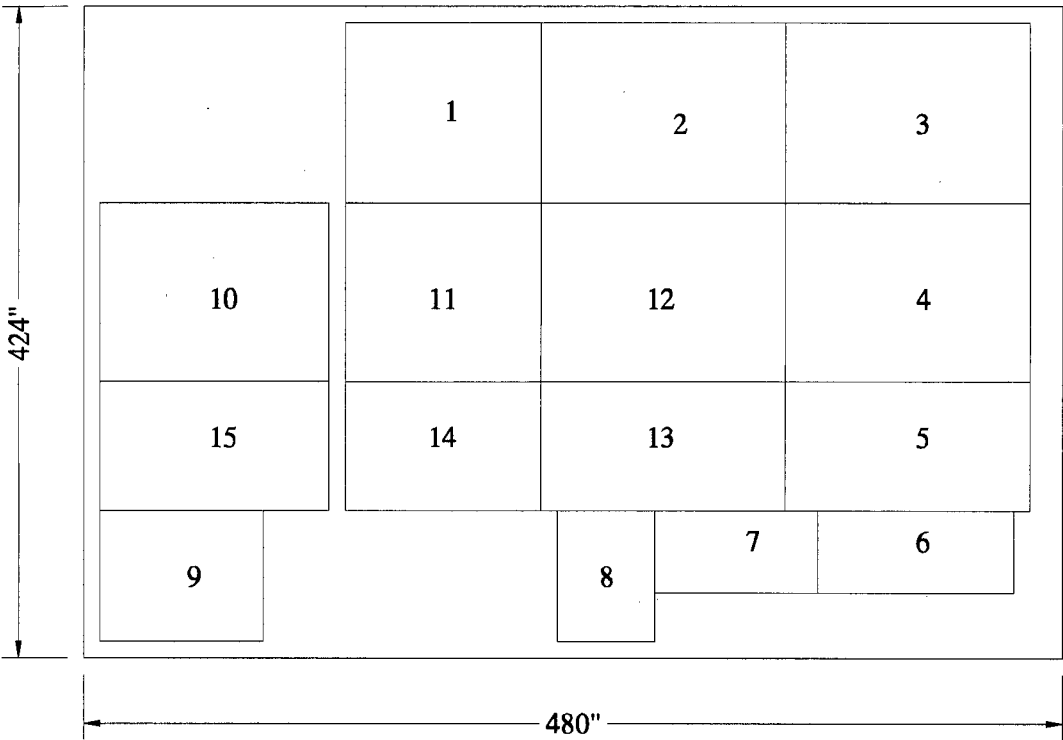


Figure 2-1: Peach Bottom Spent Fuel Pool
(Note: Numerals are RACKLIFE module designations.)

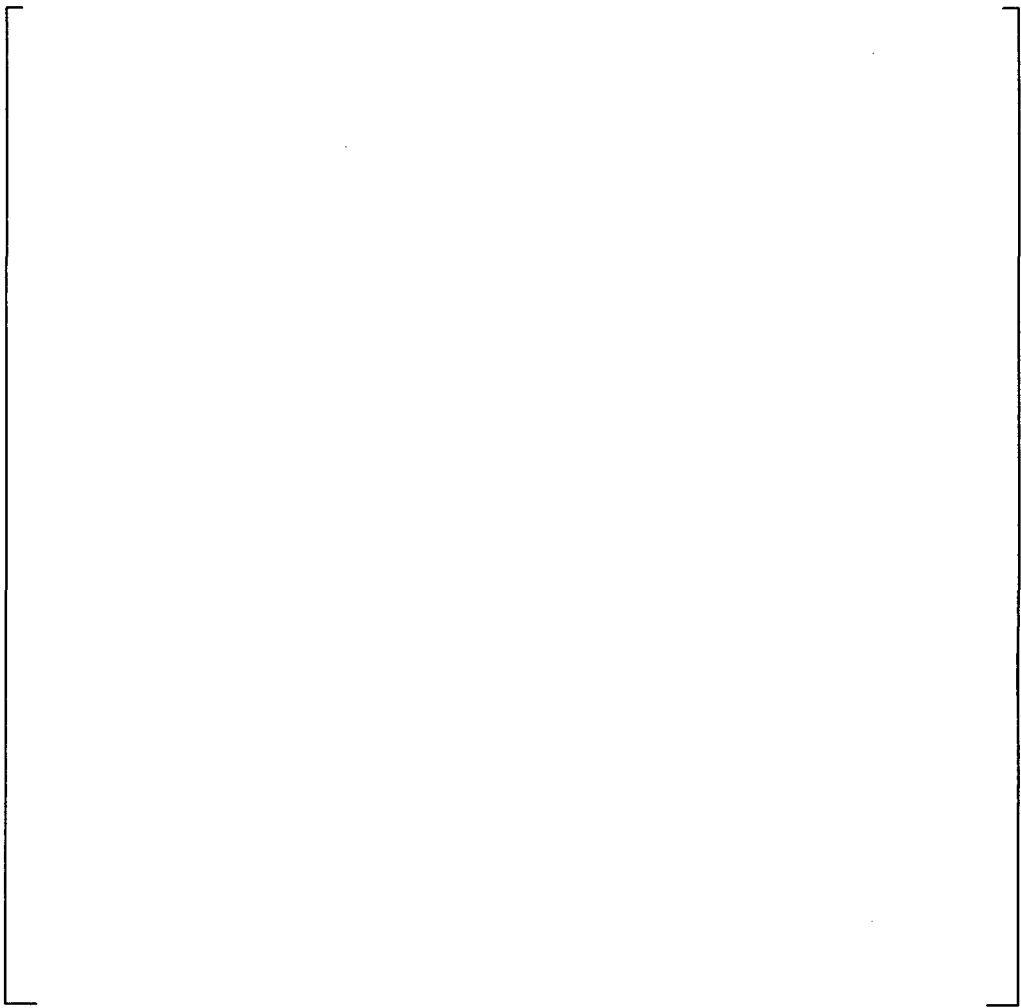


Figure 2-2: Peach Bottom Storage Cell Elements

3.0 RACKLIFE Projections

3.1 Model Overview and Assumptions

A RACKLIFE model of the Peach Bottom Unit 2 SFP was originally developed by NETCO based on data provided by Exelon^[6]. The original model was updated by Exelon to reflect subsequent fuel discharges into the spent fuel racks through February 2006. The projected dates and anticipated number of discharged assemblies for refueling outages and dry cask storage loading campaigns beyond 2006 thru 2015 were provided by Exelon^[13]. In addition, pool history data (reactive silica concentration, temperature and pH) for the Peach Bottom Unit 2 spent fuel pool were also provided. Collectively, these data were used by NETCO to update the model and project the extent of Boraflex dissolution biannually thru 2014.

This model was used to estimate the actual service history of each panel of Boraflex in the Peach Bottom Unit 2 storage racks, including integrated gamma exposure and its condition with respect to B₄C loss. Information regarding the predicted state of the pool and the condition of the Boraflex at a given time can be determined using the model.

Reactor Cycle Data

Cycle 16 ended in October 2006. All shutdowns were conservatively modeled as an instantaneous shutdown from 100 percent of rated power. Peach Bottom Unit 2 operates on a 2-year fuel cycle, and for modeling purposes it was assumed that the future refueling outages would occur in October 2008, October 2010, and October 2012 and October 2014 per the schedule provided by Exelon^[13]. Future reactor shutdowns were also modeled as instantaneous shutdown from 100 percent of rated power. This approach provides a conservative estimate of the Boraflex gamma exposure to Boraflex panels.

Fuel Assembly Data

Review of the discharged bundles currently residing in the spent fuel pool indicated that, prior to Cycle 13, all bundles were conservatively assigned a power sharing value of 1.0. Cycles 14 and 15 assembly data contain measured end-of-cycle assembly average power sharing values. These measured values were used to determine appropriate power sharing for future cycles. For Cycle 14, a weighted average end-of-

cycle power sharing of 0.74 was calculated, and for Cycle 15 the weighted average end-of-cycle power sharing was 0.63. Thus, for future offloads, discharged assemblies were conservatively assumed to have relative operating power sharing values of 0.8.

Pool History and Cleanup Data

Pool history data (temperature, pH and reactive silica concentration) were added to the pool history file. In addition, letdowns to simulate mixing of the reactor cavity water with the bulk spent fuel pool water were added to the cleanup system file to coincide with the refueling outages occurring in October of 2006, 2008, 2010 and 2012.

Assembly Shuffle and Dry Storage

Figure 3-1 shows the loading of the Peach Bottom 2 racks at the time of the test. As a result of increased plant security concerns and to satisfy the thermal management requirements of Section 2.2.54 of Exelon Procedure NF-AA-310, Rev. 9 "Special Nuclear Material and Core Component Movement", freshly discharged bundles must contain "cold" bundles on all four face adjacent cells. This requires some 1400 storage locations to accommodate a discharge batch of 276 fuel assemblies.

A major goal is to preserve Module 1 for staging reload fresh fuel as this module has seen the least severe service duty. Thus, Modules 3,4,5 and 12 were selected for placement of freshly discharged bundles. Figure 3-2 shows the projected loading pattern of the Peach Bottom Unit 2 spent fuel racks on May 1, 2010.

2

3.2 Projections through 2010

2

Using the input data and assumptions outlined in Section 3.1, the Peach Bottom RACKLIFE model was updated and executed through ISFSI campaigns of 2012 and 2014. This served to identify the cells with the greatest panel boron carbide loss and absorbed dose. Figure 3-3 shows the percent boron carbide loss for the spent fuel racks in February 2006 at the time of the last BADGER test. It can be seen that all of the panels have at least [] loss while about half of the modules have panels with more than [] percent loss. The peak loss ([]) occurs in Module 15. This calculation used an escape coefficient of 1.0/day through February 2006 and 1.25/day

2

2

beyond. The RACKLIFE model was executed iteratively by varying the "escape coefficient" until the predicted pool silica matched the measured pool silica. The escape coefficient is the rate, in units of cavity volumes (the volume of fluid in the rack cavities surrounding each Boraflex panel) per day, that are exchanged with the bulk pool volume. An increase in the slope of the measured pool silica would indicate an increase in the escape coefficient is necessary. The physical basis for this is that as the Boraflex dissolves, the clearances for flow increase, reducing the pressure drop and increasing flow.

Figure 3-4 shows there is a fairly regionalized dose distribution throughout the pool. The majority of high dose panels (greater than 1×10^{10} rads) are located in a central region of the pool in front of the transfer canal. The panels with the highest dose are the south and west panels in cell XX65 of Module 15 with an integrated exposure of 1.4×10^{10} Rads.

Prior to the End-of-Cycle 16 (EOC16), there were vacant areas in Modules 10 and 11 as well as individually scattered vacant cells in Modules 6,7,8,9,14 and 15. It was decided that discharged bundles would reside in their "B.5.b" locations for 17 months (from discharge until the subsequent ISFSI campaign) and then be moved to a vacant module. For the 2006 offload, B.5.b cell locations were vacated and resident bundles moved to Modules 10 and 11. In 2008, Module 11 was vacated and all bundles moved into dry storage casks. Bundles discharged in 2006 were subsequently moved to cells in Module 11. In 2010, bundles in Module 10 were "moved into dry storage" and B.5.b cell locations vacated with bundles discharged in 2008 relocated to module 10. The same process was repeated for the 2012 ISFSI campaign, with bundles in Modules 14, 15 and part of Module 9 being placed into dry storage.

2

Figure 3-5 shows the distribution of panel boron carbide loss for the Peach Bottom spent fuel racks to May 1, 2010. The average panel boron carbide loss is [] percent with a standard deviation (1σ) of [] percent. The maximum panel loss is [] percent to May 1, 2010.

2

Figure 3-6 shows the distribution of panel absorbed dose (Rads) for the Peach Bottom spent fuel racks to May 1, 2010. The average absorbed dose to all panels in the Peach Bottom spent fuel pool is 5.2×10^9 Rads, while the maximum projected panel absorbed dose is 1.5×10^{10} Rads.

2

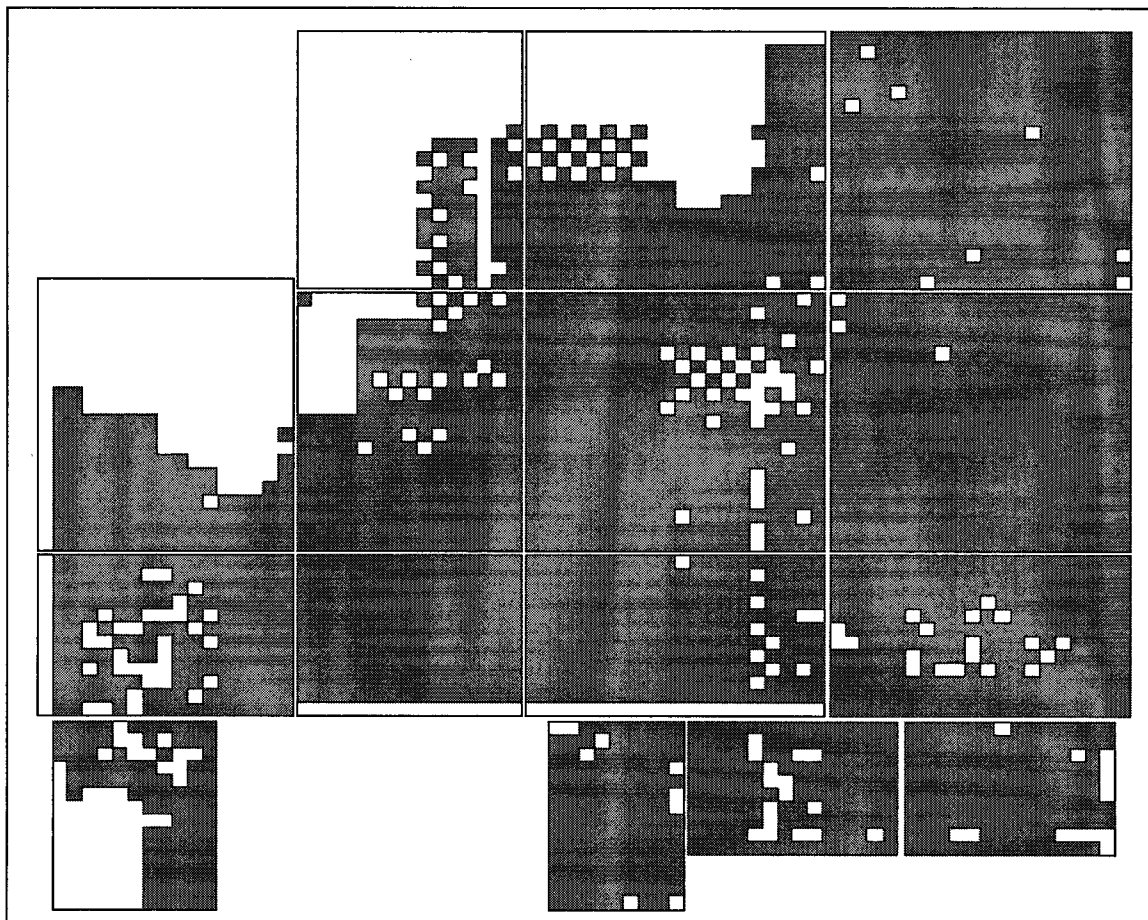
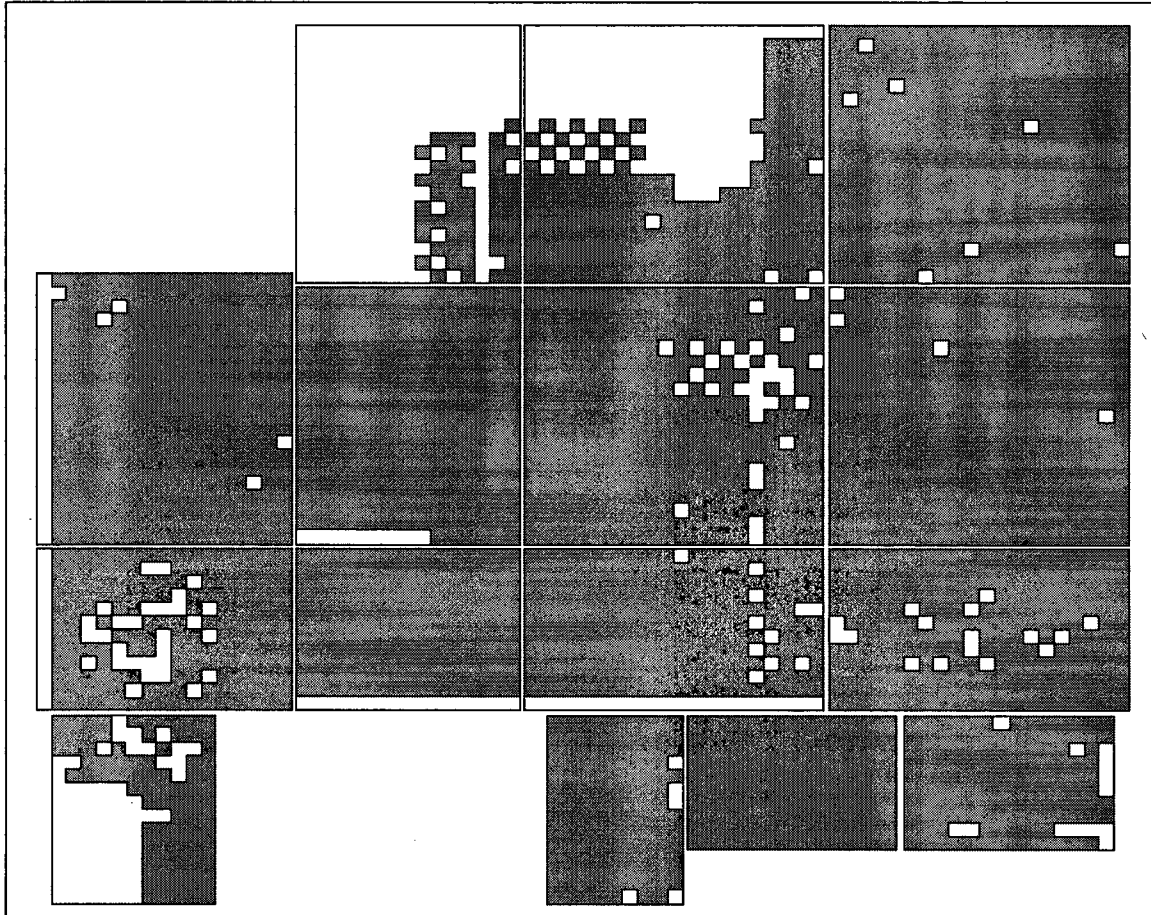


Figure 3-1: Occupied Cells in the Peach Bottom 2 Spent Fuel Storage Racks on February 26, 2006.



2

Figure 3-2: Projected Occupied Cells in the Peach Bottom 2 Spent Fuel Storage Racks on May 1, 2010.



Figure 3-3: Predicted Boron Carbide Loss through February 26, 2006 in the Peach Bottom Spent Fuel Storage Racks

Key:

- Red: > 18% loss
- Yellow: > 12% loss
- Green: > 6% loss

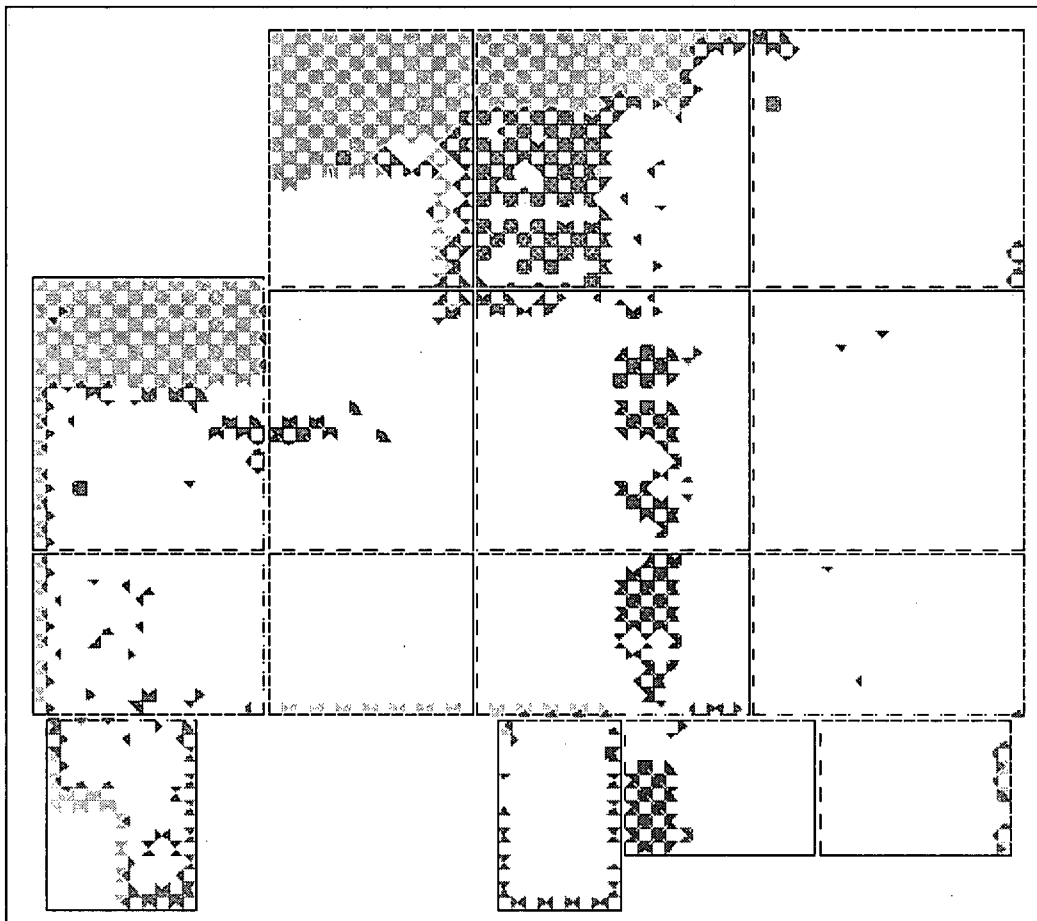


Figure 3-4: Panel Absorbed Dose through February 26, 2006 in the Peach Bottom Spent Fuel Storage Racks

Key:

- Red: $> 1 \times 10^{10}$ Rads
- Yellow $> 2 \times 10^9$ Rads
- Green $> 5 \times 10^8$ Rads

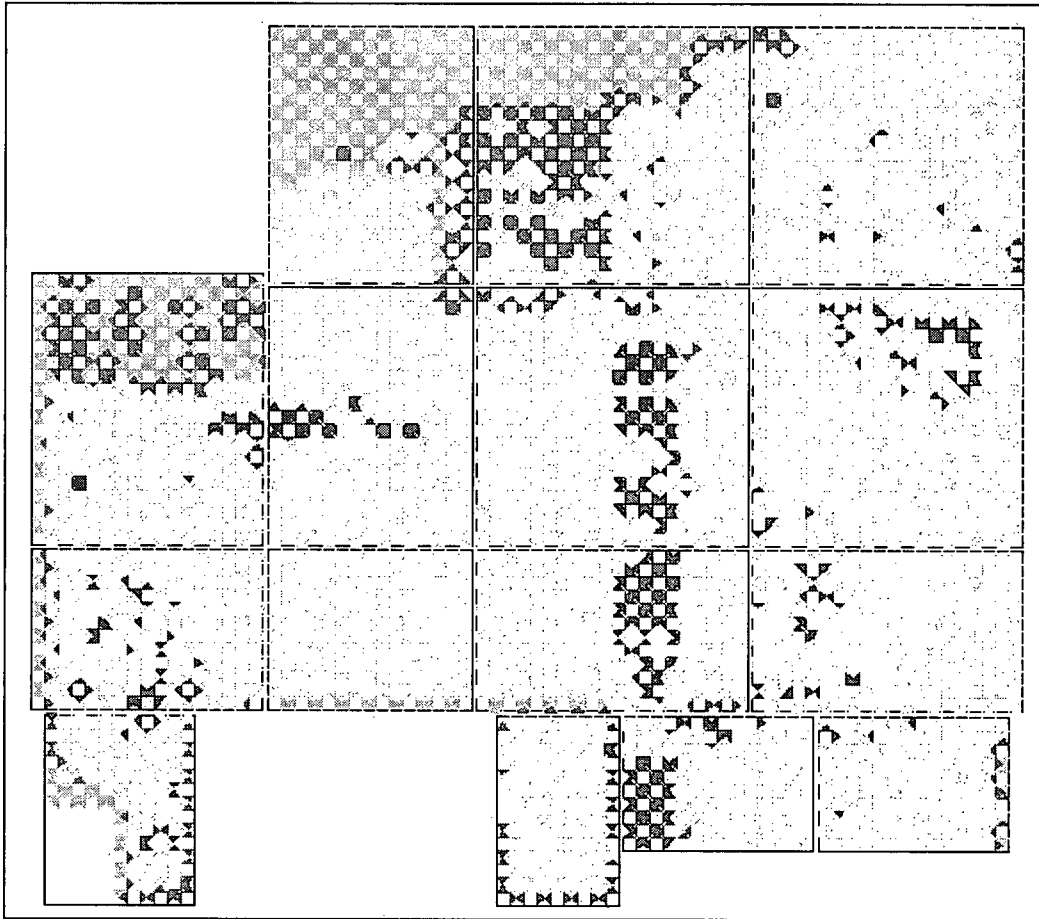


2

Figure 3-5: Predicted Boron Carbide Loss through May 1, 2010 in the Peach Bottom Spent Fuel Storage Racks

Key:

- Red: > 27% loss
- Yellow: > 18% loss
- Green: > 9% loss



2

Figure 3-6: Panel Absorbed Dose through May 1, 2010 in the Peach Bottom Spent Fuel Storage Racks

Key:

- Red: $> 1 \times 10^{10}$ Rads
- Yellow $> 2 \times 10^9$ Rads
- Green $> 5 \times 10^8$ Rads

4.0 The Reactivity Effects of Boraflex Degradation

4.1 Introduction

This section examines the reactivity effects of Boraflex panel degradation in the Peach Bottom Unit 2 spent fuel racks. Boraflex panel degradation can be divided into three modes, which are characterized by different degradation mechanisms, as described below.

4.1.1 Uniform Dissolution

As described in Section 2.0, the Boraflex panels in the Peach Bottom Unit 2 spent fuel racks are contained in a "panel cavity" created between the [] inch thick stainless steel cell wall, and the [] inch thick stainless steel wrapper plate. The void volume of this panel cavity is filled with water that generally surrounds the Boraflex panel. The exchange of fluid between the bulk pool and the panel cavity (as measured by the "escape coefficient") results in a flow across the surfaces of the Boraflex panel as well as local flow paths in between the tack welds long the wrapper plate. This can lead to a relatively uniform dissolution of the amorphous silica from Boraflex panel surfaces along with local scallop regions and consequent loss of absorber.

This mode of degradation increases the transmission of neutrons between assemblies in the spent fuel racks by decreasing the amount of intervening absorber. However, the remaining absorber still interposes between assemblies.

4.1.2 Shrinkage, Including Gaps

Radiation induces crosslinking of the polymer matrix of Boraflex. This causes the material to shrink, reducing the volume of a Boraflex panel. While shrinkage reduces the volume of an interposing panel, shrinkage does not reduce the mass of interposing absorber, that is, the material undergoes densification as it shrinks.

Width and end shrinkage can “uncover” the active fuel, allowing direct neutron transport between assemblies without any intervening absorber. If a Boraflex panel is not allowed to shrink uniformly (e.g., it is mechanically restrained), gaps will develop. This can lead to direct neutron transport between the centers of assembly faces.

4.1.3 Local Dissolution

The dissolution described as mode 1, above, is generally uniform. However, local non-uniformities in the panel, panel cavity, and cavity inlet/outlet geometry can accentuate dissolution locally. For example, a gap in a panel locally increases the cavity volume, which locally reduces the effects of wall friction on flow. This can increase local flow rates causing accelerated dissolution. As another example, a bend, bow, or creases in the stainless steel wrapper plates can provide the orifices, allowing increased flow into or out of the panel cavity, thereby accelerating local degradation. These local effects can exhibit a positive feedback; they accelerate the local dissolution of Boraflex, which increases the local cavity volume. This in turn decreases wall friction losses, increasing local flow rates, further accelerating local Boraflex dissolution.

As suggested in the discussion for each mode of dissolution, each mode will affect the spent fuel pool reactivity differently. These synergistic reactivity effects may be strongly non-linear. Criticality safety calculations using highly bounding assumptions, (e.g., very large gaps all at the assembly mid-plane, complete dissolution of the Boraflex, etc.) lead to reactivity increases far in excess of the actual reactivity state of the spent fuel pool. On the other hand, the non-linear synergy necessitates a robust analysis of the degradation, in order to conservatively take some credit for the Boraflex that remains in the racks. This section of the report outlines a methodology for such a robust analysis.

4.2 Methodology for Projecting Future Panel Conditions

The results of the latest BADGER test campaign at Peach Bottom Unit 2^[8] were used to characterize the state of the Peach Bottom Unit 2 spent fuel racks Boraflex panels at

the time of testing. The RACKLIFE projections (discussed in Section 3) were further used to conservatively project the state of the panels to May 1, 2010.

| 2

Algorithms were developed for randomly sampling panel local degradation features based on the BADGER data. The input to the algorithms are the panel absorbed dose and B₄C loss predicted by RACKLIFE. The algorithms are based on random sampling from probability distributions of loss versus absorbed dose developed from the observed BADGER data. The use of normal and uniform random numbers in the algorithms account for the variance observed between RACKLIFE predictions and BADGER observations and the random nature of local dissolution effects.

The Boraflex panel models developed represent degraded panels conservatively projected to May 1, 2010. They consist of an array of rectangular blocks: four blocks across a panel to match the four detectors in BADGER, and each block two inches high to match the two-inch “window” in front of the BADGER detectors. Away from local areas of dissolution the blocks are as thick as a nominal panel of Boraflex. Each panel of Boraflex in the Peach Bottom Unit 2 spent fuel racks that was measured by BADGER was characterized using this system of blocks. Figure 4-1 is an example of a panel model. In Figure 4-1, the column heading “Elev” refers to the axial elevation of each block center. (The panel shown represents a [] inch panel; note that the panel is displayed top to bottom.) The columns are numbered to correspond to the four BADGER detectors and represent an area of the panel 1.23 inches wide by 2 inches high.

| 2

| 3

Integer values in Figure 4-1 represent an amount of gap in a block in thirds of an inch. Thus the row of “2”s on a red background indicates a two-thirds inch gap at an elevation of 43 inches. Cells in the panel model that are not colored are at a specified level of uniform loss. The values on blue backgrounds represent areas of local dissolution, quantified by the percent loss from the uniform loss condition. Some of the dissolution occurs around the gap, some near the end of the panel, and some independent of any other features of the panel. Dissolution that occurs around a feature is assumed to

extend into the feature. For example, the []% loss measured by detector 2 (column 2) at 131 inches is assumed to persist in the column 2 cell at 133 inches. In reality, BADGER would detect the additional loss if it was there, but this accounts for any uncertainty in an analyst's interpretation of how to allocate the loss. In the case of the gap at 43 inches, a loss of []% is assumed under detectors 3 and 4 since this is (conservatively) the largest loss proximal to the gap.

In applying the panel models to the state of the Peach Bottom Unit 2 spent fuel racks in 2010, the degree of conservatism used is best illustrated by the following examples. | 2

Example 1: Loss Equivalence

The BADGER campaign at Peach Bottom Unit 2 in February 2006 measured the state of the Peach Bottom Unit 2 spent fuel rack Boraflex panels at that time. The RACKLIFE code was used to identify which panels in the Peach Bottom SFRs had the highest absorbed dose and/or the highest predicted B₄C loss. Measurements were performed on panels with a spectrum of dose and loss (in order to observe and quantify any trends with dose and loss), but with a strong bias toward the "worst" panels. Therefore, the panels that BADGER measured are typical of the worst panels in the pool. During the BADGER campaign in February 2006, 38 panels exhibited a measurable loss of boron carbide. The average loss from these 38 panels was []%±[]%.

On May 1, 2010, RACKLIFE predicts that the average loss for all panels in the racks is []% ±[]%. These losses are comparable to what BADGER measured for the panels that actually exhibited a loss. For example, in predicting the condition of a 20% loss panel in 2010, it is reasonable to assume that the condition would be equivalent to a 20% loss panel as measured by BADGER in 2006. If a 20% loss panel is not available, then the next higher loss panel measured is conservatively used. In this manner, projected panels in 2010 can be conservatively loss-equivalenced to panels measured by BADGER in 2006. | 2
| 2
| 2
| 2

Example 2: Loss Extrapolation

On May 1, 2010, RACKLIFE predicts that the average loss in the racks is [] ± []%, with a maximum loss of []. The average loss measured by BADGER (for all panels in 2006) was []%. None of the panels exceeded the maximum loss predicted by RACKLIFE. Of the three modes of degradation described in Section 4.1, the first two, uniform dissolution and shrinkage, can be conservatively projected with a fair degree of confidence and precision. The degradation mechanisms are well understood and bounding models can be formulated. The third mode, local dissolution, however, is random in nature and is not as amenable to prediction.

2 | 3

For example, consider a typical local dissolution feature: a “scallop” in the side of the panel where higher levels of loss are observed. As illustrated below, suppose this takes the form of two 2” high by 1.23” wide rectangular cells along the left edge of the panel with 30% more loss than the uniform loss of the bulk panel. (The rectangular cells bound the actual size and shape of the scallop.)



The question is, more specifically now, what will this local dissolution feature look like in a panel that has undergone 1.5 times as much dissolution? Three distinct degradation scenarios can be considered: 1) the scallop increases in size by a factor of 1.5 (to three cells instead of two); 2) the scallop “deepens” by a factor of 1.5 (from 30% loss to 45% loss); or 3) the scallop remains the same and another one-cell scallop with 30% loss develops somewhere else on the panel. The truth is likely a randomly weighted mixture of all three modes. To select a bounding degradation scenario is virtually impossible,

since the reactivity effects of each scenario will depend on the elevation of the scallop, its proximity to other local dissolution features, gaps or end shrinkage. The conservative approach used was to assume all three scenarios occur simultaneously on a cell-by-cell basis. As a conservative upper-bound, the next highest (worse) local dissolution pattern for the scallop was then selected.

Using the panel projections described above, the methodology described in section 4.3 was developed for simulating the reactivity effects of Boraflex panel degradation.

4.3 Methodology for Assessing the Reactivity Effects of Boraflex Degradation

The methodology described below was applied to the Peach Bottom Unit 2 spent fuel racks. For clarity, the description below will generally refer to the racks generically.

The SCALE code package (described in Section 5.2) was used to calculate k_{eff} for the racks. For the reactivity equivalence model, the Boraflex was assumed to be at its nominal thickness and ^{10}B loading. In addition, a conservatively bounding 4.1% width shrinkage was also applied. This bounding shrinkage is based on both analytical and experimental analyses^[2] and has been confirmed by a large number of proprietary laboratory studies and field observations. Recall from Section 4.1 that thickness shrinkage is effectively offset by densification and so need not be accounted for. As described in Section 4.1, the effects of axial shrinkage manifest themselves as both end shrinkage and gapping. Measuring the amount of shrinkage-induced gapping is complicated by the fact that local dissolution can increase the apparent size of a gap. Further, BADGER may miss gaps that are less than 1/3rd inch or smaller. To account for the axial shrinkage with the possibility that some gaps may have been missed, it is conservatively assumed that every panel has an undetected 4.1% axial shrinkage in the form of 1/3rd inch gaps uniformly distributed up the panel. The reactivity effect of this assumption is shown in Table 4-1. These assumptions result in a higher than nominal reactivity model, which conservatively increases the reactivity effects of Boraflex loss.

The Boraflex thickness in the base model was then uniformly decreased in 5% increments to observe the reactivity effects of uniform dissolution. The results were used to develop a relationship between uniform thinning and an increase in k_{eff} for reactivity equivalencing between pure uniform thinning and the actual degraded condition of the Boraflex. The results are shown in Table 4-2.

Next, a verified and validated Fortran program was used to modify the base case, so that every panel in a given array of rack cells could be modeled independently. The algorithms described in Section 4.2 were used to create panel models as described in that section for each panel in the array. For this analysis, a [] array of cells was modeled, thus, a total of [] panels are generated by the algorithm according to the dose and loss predicted by RACKLIFE for each panel. These degraded models of Boraflex panels are incorporated into a KENO model to simulate the conditions of the module in 2010. This case is used to calculate a single estimate of the reactivity effect of Boraflex panel degradation in the Peach Bottom Unit 2 spent fuel racks in 2010.

3
3
2

In executing the case, a total of 30 million neutrons were tracked over 3000 generations. Fifty generations were skipped to ensure convergence of the source distribution. The large number of neutrons was used to ensure that there was adequate sampling of all of the degradation features of all of the panels in the model. As per standard practice, plots and statistics of the evolution of k_{eff} by generation were inspected and calculated to provide confidence that no sampling instabilities were being encountered.

As described in Section 4.2, the Boraflex panels generated for a model were based on a sequence of random numbers, so that each panel model is a random model with an expected value defined by the BADGER measurements plus a random variance. Consequently, the single estimate case described above could be randomly higher or lower than the actual condition of the panel being modeled. Therefore, a total of [] independent and randomly distributed cases were created using the Fortran program. These cases resulted in a distribution of calculated reactivity effects. The 95th percentile

3

of this reactivity effects distribution, at 95% confidence, can be used to bound the reactivity effects of degraded Boraflex panels in the array of cells being considered. Figure 4-2 shows one example of this distribution as points in a cumulative distribution with the Monte Carlo statistical uncertainty, as shown by the error bars. The line in Figure 4-2 is a cumulative normal distribution with a mean and variance from the [] | 3 samples. In every distribution calculated, the data passed the Anderson-Darling and Cramér-von Mises tests for normality; thus, one-sided normal distribution statistical tolerance factors are valid for calculating bounding 95th percentile eigenvalues at 95% confidence. Figure 4-2 shows that [] samples are sufficient to bracket the 95th | 3 percentile and to look for any potential non-normal behavior in the tails. No non-normal behavior was observed.

4.4 Results

Table 4-3 summarizes the reactivity effects in the Peach Bottom Unit 2 spent fuel racks. The RACKLIFE predicted loss, as a uniform thinning loss, is shown in column 1. The RACKLIFE code does not distinguish between uniform loss and local dissolution losses. The reactivity effect in column 2 is the 95th percentile effect at 95% confidence and includes the effects of uniform dissolution, local dissolution, and gaps.

Table 4-2 was used to interpolate the equivalent amount of uniform thinning loss that will yield the same reactivity effect as the 95/95 effect above. The results are shown in column 2. The value of [] for the equivalent loss in the racks is a conservative | 2 | 3 over-estimate of the actual equivalent loss. Most of the panels measured by BADGER in 2006 had very low losses compared to the losses predicted for the population of panels. Thus, in equivalencing observed panel losses with predicted losses, a large amount of conservatism was introduced for the low loss panels.

Column 4 shows the conservative amount of uniform thinning loss that will be assumed in subsequent analyses. The many conservatisms used to arrive at these numbers provides confidence that these losses will bound the state of the Peach Bottom Unit 2 spent fuel racks, on May 1, 2010. | 2

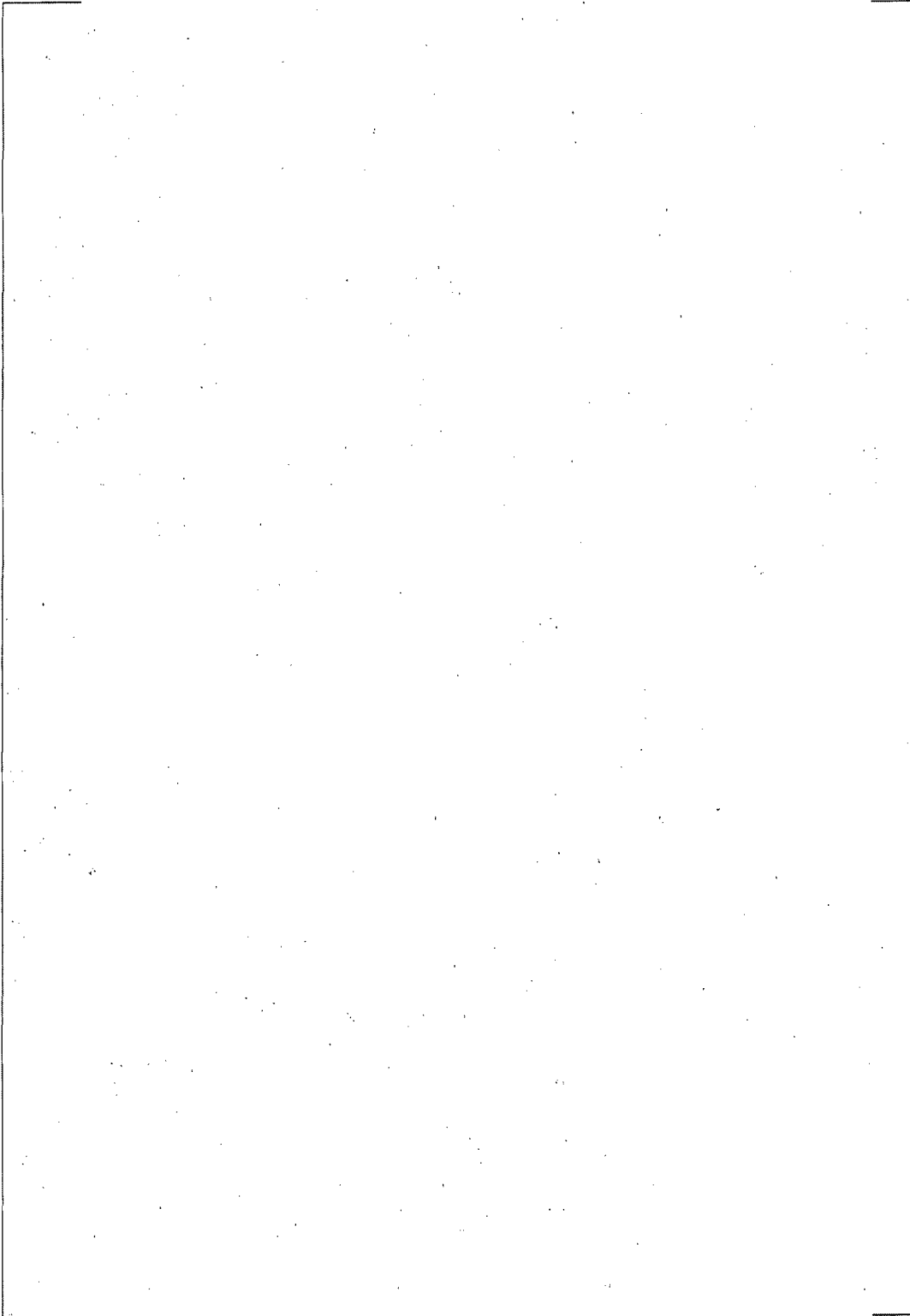


Figure 4-1: Typical Model of an Peach Bottom Unit 2 Boraflex Panel



Figure 4-2: Sample Distribution of Panel Degradation Reactivity Effects

5.0 Results of the Criticality Analysis

The criticality analyses and evaluations described in this report demonstrate that the k_{eff} of the Peach Bottom Unit 2 spent fuel racks is less than or equal to 0.95 when loaded with the most reactive (GNF 2) fuel types under the most reactive conditions. The maximum calculated reactivity (k_{eff}) when adjusted for computer code biases, fuel and rack manufacturing tolerances and methodology/calculational uncertainties (combined using the root-mean-square method) will be less than or equal to 0.95 with a 95% probability at a 95% confidence level.

5.1 Design Basis and Design Criteria

All analyses and evaluations have been conducted in accordance with the following codes, standards and regulations as they apply to spent fuel storage facilities:

- American Nuclear Society, American National Standard Design Requirements for Light Water Reactor Spent Fuel Storage Facilities at Nuclear Power Plants, ANSI/ANS-57.2-1983. October 7, 1983.
- Nuclear Regulatory Commission, Letter to All Power Reactor Licensees from B. K. Grimes. *OT Position for Review and Acceptance of Spent Fuel Storage and Handling Applications*. April 14, 1978, as amended by letter dated January 18, 1979.
- Nuclear Regulatory Commission, memorandum from Laurence Kopp to Timothy Collins. *Guidance on the Regulatory Requirements for Criticality Analysis of Fuel Storage at Light-Water Reactor Power Plants*. August 19, 1998.
- USNRC Standard Review Plan, NUREG-0800, Section 9.1.1, New Fuel Storage, and Section 9.1.2, Spent Fuel Storage.
- USNRC Regulatory Guide 1.13, Spent Fuel Storage Facility Design Basis, Rev. 2, March 2007.
- USNRC Regulatory Guide 3.41, Validation of Calculational Methods for Nuclear Criticality Safety.

NET-264-02 NP
Non-Proprietary Information Submitted in
Accordance with 10 CFR 2.390

- General Design Criterion 62, Prevention of Criticality in Fuel Storage and Handling.

- ANS/ANSI 8.12-1987, Nuclear Criticality Control and Safety of Plutonium - Uranium Fuel Mixtures Outside Reactor.

It is noted that the above USNRC and ANS documents refer to the requirement that the maximum effective neutron multiplication factor (k_{eff}) is to be less than or equal to 0.95. In demonstrating that this requirement is satisfied, the analyses herein of the reference (nominal dimensions) case fuel/rack configurations are based on an infinite repeating array in all directions. A bias (credit) for axial leakage is applied to the reference calculation based on a model which is finite in the z-direction.

5.2 Analytical Methods and Assumptions

This analysis utilizes the stochastic three dimensional Monte Carlo code KENO V.a^[14] and the two dimensional deterministic code CASMO-4^[15] to compute the reactivity effects due to degraded Boraflex. The CASMO code yields a deterministic solution to the neutron transport equation, which is useful for precisely computing reactivity changes. The stochastic nature of the Monte Carlo solution in KENO means that statistical tolerance factors at 95% probability with 95% confidence must be applied to the solution. On the other hand, CASMO is limited to two-dimensional (axially uniform) single cell (infinitely reflected) models, while KENO provides robust three-dimensional modeling capability. Thus, KENO is used when axial effects are important (e.g., axially distributed gaps), or when lateral non-uniformities are present (e.g., checkerboard loading).

KENO V.a is a module in SCALE 5.0, a collection of computer codes and cross section libraries used to perform criticality safety analyses for licensing evaluations. KENO solves the three-dimensional Boltzmann transport equation for neutron-multiplying systems. The collection also contains BONAMI-S to prepare problem specific master cross section libraries and to make resonance self-shielding corrections for nuclides with Bondarenko data. NITAWL-II is used to prepare a working cross section library with corrections for resonance self-shielding using the Nordheim integral treatment. These modules are invoked automatically by using the CSAS25 analysis sequence in SCALE 5.0.

CASMO-4 is a two dimensional multigroup transport theory code for fuel assembly burnup analysis in-core or in typical fuel storage racks. CASMO is a cell code in which infinitely repeating arrays of fuel assemblies and/or fuel racks are modeled.

These codes have been verified and validated for use in spent fuel rack design evaluations by using them to model a number of critical experiments^[15-19]. The results of this validation and verification are included in this report as Appendix A^[20]. The calculated k_{eff} was compared to the critical condition ($k_{\text{eff}} = 1.0$) to determine the bias in the calculated values.

In all SCALE/KENO calculations the 238 energy group ENDF/B-V criticality safety cross section library^[21] was used. The resulting bias in the SCALE codes was calculated to be []. In all CASMO calculations, the CASMO standard 70 energy group cross section library was used. In all CASMO-4 calculations, the 70-energy group neutron library^[15] was used. The resulting bias in the CASMO-4 code was calculated to be []. The 95/95 statistical one-sided tolerance factor is $\kappa \approx 4.19$.^[22]

2

As noted above, all KENO results require that a one-sided 95% probability / 95% confidence statistical tolerance factor be applied to the computed eigenvalue. In all KENO runs, typically 3000 generations (after skipping 50 for source distribution convergence) with between 2000 and 3,000 neutrons per generation were simulated for a total of between 6 million to 9 million neutrons tracked. This typically resulted in statistical uncertainties in k_{eff} of $\sigma < 0.0003$ (one standard deviation) and a 95/95 statistical tolerance factor $\kappa \approx 2.05$.^[22]

2

The depletion characteristics of GNF 2 bundle (k_{∞} versus burnup) in both the core geometry and fuel rack geometry have been assessed with CASMO-4 to determine the burnup resulting in peak bundle reactivity (k_{∞}). In these calculations the fuel bundle is depleted at hot full power conditions in core geometry using CASMO-4. At specified burnup steps the bundle is brought to the cold zero power condition (no Xenon) and modeled in the rack geometry. Subsequently, the bundle is subjected to additional burnup in the hot full power condition in core geometry and the process repeated.

NET-264-02 NP
Non-Proprietary Information Submitted in
Accordance with 10 CFR 2.390

The design point for the Peach Bottom 2 fuel racks is taken at the burnup corresponding to peak reactivity of the Gd_2O_3 bearing maximum reactivity bundle. A bias to account for depletion uncertainties is added to the k_{∞} at the point of peak reactivity to account for uncertainties in the depletion dependent cross sections.

To assure that the actual fuel/rack reactivity is always less than the calculated maximum reactivity, the following conservative assumptions have been applied to the analyses:

1. The fuel assembly design parameters for these analyses are based on the most reactive 10 x 10 fuel types.
2. The maximum fuel enrichment is [] w/o U^{235} with gadolinia and is assumed to be uniform throughout the bundle. The assumption of uniform enrichment results in a higher reactivity than would the distributed enrichment, which actually exists in the bundles.
3. The fuel bundle includes a coolant flow channel in the rack as this condition results in the highest reactivity.
4. The moderator is assumed to be demineralized water at full water density (1.0 gm/cm^3).
5. The array is infinite in lateral extent (x , y and z directions). A reactivity credit for axial neutron leakage is subsequently applied to the reference eigenvalue. Non-conservative, but appropriate.
6. All available storage locations are loaded with bundles of maximum reactivity.
7. No credit is taken for neutron absorption in the fuel assembly grid spacers.
8. No credit is taken for any natural uranium or reduced enrichment axial blankets.
9. Boraflex is assumed to be uniformly at []% nominal thickness (i.e., []% Uniform Thinning Loss). Tolerances were conservatively evaluated at 35% uniform thinning.

2

Based on the analyses described subsequently the maximum k_{eff} of the fuel/rack configuration at a 95% probability with a 95% confidence level is calculated as:

$$k_{eff} = k_{ref} + \Delta k_{bias} + \sqrt{\sum_{n=1}^{15} \Delta k_n^2}$$
2

where

k_{ref}	=	Nominal k_{eff} adjusted for depletion effects	
Δk_{bias}	=	$\Delta k_{method} + \Delta k_{self-shielding} + \Delta k_{undetected\ cracks} + \Delta k_{Leakage}$ $+ \Delta k_{geometry}$	2

Tolerances and Uncertainties:

Δk_1	=	UO ₂ enrichment tolerance	
Δk_2	=	UO ₂ pellet density tolerance	
Δk_3	=	Gd ₂ O ₃ loading tolerance	
Δk_4	=	Rack cell pitch tolerance	
Δk_5	=	Rack cell wall thickness tolerance	
Δk_6	=	Asymmetric assembly position tolerance	
Δk_7	=	Boraflex panel width tolerance	
Δk_8	=	Boraflex B-10 loading tolerance	
Δk_9	=	Channel bulge effect	
Δk_{10}	=	Keno V.a Methodology bias uncertainty (95/95)	2
Δk_{11}	=	Monte Carlo calculation uncertainty (95/95)	
Δk_{12}	=	Burnup uncertainty	
Δk_{13}	=	Pellet diameter tolerance	
Δk_{14}	=	Clad thickness tolerance	
Δk_{15}	=	CASMO Methodology bias uncertainty (95/95)	

5.3 Calculated Results

5.3.1 Reference Eigenvalue Calculations

The fuel racks have been analyzed for GNF 2 fuel with a maximum average planar enrichment of [] w/o U-235 and a minimum of [] Gd₂O₃ rods with a minimum loading of [] w/o Gd₂O₃. The fuel design parameters for the GNF 2 fuel assembly are summarized in Table 5-1.

3

CASMO-4 was applied to compute the reactivity of the GNF 2 fuel type as a function of burnup for bundles with [] gadolinia rods @ [] w/o gadolinia and for bundles without Gd₂O₃. Figure 5-1 contains a plot of rack k_∞ versus burnup for the GNF 2 fuel bundle. As shown in this figure the GNF 2 fuel bundle with Gd₂O₃ has a peak reactivity of k_∞ = [] which occurs at [] GWD/MTU.

2

This bias corrected peak reactivity, k_∞ = [], was calculated using CASMO. As such, the geometric limitations of this infinite array two-dimensional criticality code did not permit explicit modeling of the asymmetries of the PB2 spent fuel racks. A KENO V.a model which mirrored the CASMO-4 geometry was created. The model is infinite in the x,y,z directions with no gadolinia at a reactivity fresh fuel enrichment (REFFE) that has been determined to be equivalent to the reactivity of the same bundle depleted by CASMO-4 up to the burn-up at peak reactivity. See Figure 5-1. Using this KENO V.a model of the CASMO-4 geometry, KENO V.a was executed several times while iterating on U²³⁵ enrichment to determine the REFFE that resulted in a k_∞ = []. This corresponds to an REFFE of [] weight percent U²³⁵. To further illustrate the fidelity between CASMO and KENO V.a calculations, a zero burn-up comparison between the CASMO-4 and the KENO V.a models was performed. The difference in respective k_∞ values was determined to be negligible [], however, this is included as a reactivity bias.

2

To quantify the geometric effects of the CASMO simplified geometry, a KENO V.a “exact geometry” model of the PB2 spent fuel rack was created. This model was used to approximate the difference in k_∞ value so calculated with the k_∞ value calculated using the “CASMO-4 geometry.” The calculated difference was Δk = []. This value of geometry bias was applied to the peak CASMO-4 calculated value of k_∞, to determine the in-rack peak reactivity of k_∞ = [].

Table 5-1

**GNF 2 Fuel Assembly Description
Peach Bottom Nuclear Generating Station**



2



Figure 5-1: Rack Reactivity versus Burnup for the GNF 2 Fuel Type in the Peach Bottom Unit 2 Spent Fuel Storage Racks.

5.3.2 CASMO-4 and KENO V.a Reactivity Calculations in Core and in Rack Geometries

As a check of the two independent methods used for these analyses, the reactivity of the GNF 2 fuel types in the standard core geometry at cold conditions (68° F) have been calculated with both KENO V.a and CASMO-4 at zero burnup. Table 5-2 contains the core k_{∞} for the GNF 2 bundles with and without Gd_2O_3 rods. The reported values include model biases, which have been determined via benchmark calculations. These biases are [] and [] for KENO V.a and CASMO-4, respectively. Table 5-3 contains a similar comparison of the Peach Bottom rack k_{∞} as calculated with KENO V.a and CASMO-4.

2

Table 5-2

**CASMO-4/KENO V.a Reactivity Comparison in Core Geometry:
 GNF 2 Bundles @ [] w/o U-235 ([]% T.D.), Zero Burnup**

--	--

2

Table 5-3

**CASMO-4/KENO V.a Reactivity Comparison in Rack Geometry:
 GNF 2 Bundles @ [] w/o U-235 ([]% T.D.), Zero Burnup**

--	--

2

In addition, the k_{∞} at peak reactivity in the Standard Cold-Core Geometry (SCCG) as calculated by CASMO-4 was [].

2

The small differences in the eigenvalues are likely attributable to small differences in cross sections. This comparison serves to confirm the calculational methods.

5.3.3 Effect of Tolerances and Uncertainties

Tolerances and Calculational Uncertainties

To evaluate the reactivity effects of fuel and rack manufacturing tolerances, CASMO-4 and Keno V.a perturbation calculations were performed. The most reactive GNF 2 fuel bundle (with Gd_2O_3) at a burnup of [] GWD/MTU was used. The following tolerance and uncertainty components are addressed, based upon 35% uniform thinning:

2
2

U-235 Enrichment: The enrichment tolerance of \pm [] w/o ([]% relative) U-235 variation about the nominal reference value of [] w/o U-235 was considered^[11].

UO₂ Stack Density: An upper tolerance level of $\pm 0.50\%$ about the nominal reference theoretical density of []%^[11] was assumed. (Note: this tolerance effect was not included in the Reference 11 analysis.)

Pellet Dishing: The pellets were assumed to be undished. This is a conservative assumption in that it maximizes the U-235 loading per axial centimeter of the fuel stack. No sensitivity analyses were completed with respect to the variations in the pellet dishing factor.

Gd₂O₃ Loading: The tolerance of \pm []% (relative) has been assumed (Note: This tolerance effect was not included in the Reference 11 analysis).

Cell-to-Cell Pitch: The manufacturing tolerance of \pm [] inches for the variations in cell-to-cell pitch was used^[11].

Stainless Steel Thickness: A stainless steel sheet tolerance of \pm [] inches consistent with previous analyses was used^[11].

Boraflex Width: A manufacturing tolerance of \pm [] inches on the Boraflex width was assessed. The Boraflex material is replaced with water at maximum density.

Boraflex Loading: A manufacturing tolerance of \pm [] gm B¹⁰/cm² was used based on a review of Boraflex batch records^[6].

Boraflex Thickness: As described in Section 4.3, the reactivity effect due to density increase from shrinkage offsets the small effect of a reduction in thickness tolerance.

Pellet Diameter: A manufacturing tolerance of [] inches was considered.

2

Clad Thickness: A manufacturing tolerance of [] inches was considered.

The reactivity effects of combined local dissolution, shrinkage induced gaps and uniform thinning are equivalent in reactivity to a uniform panel thinning of []%. It was conservatively assumed that the panel thickness was at []% of the nominal thickness ([]). This effect is modeled in the base eigenvalue (k_{ref}).

2

Assembly Location: The reference CASMO reactivity calculations are based on a model with each bundle symmetrically positioned in each storage cell. The effect of four adjacent assemblies with minimum separation distance has been considered and has a small effect ([]) on reactivity.

Methodology Uncertainty: The 95% probability/95% KENO V.a confidence level uncertainty of [] and the 95% probability/95% confidence level CASMO-4 uncertainty of [] as determined from benchmark calculations (see Appendix A) have been applied. These uncertainties contain the one-sided tolerance factors as discussed in Section 5.2. The result of these analyses of the reactivity effect of tolerances is contained in Table 5-4.

2

Channel Bulge: The effect of channel bulge was analyzed to determine its impact or reactivity relative to the reference case model of an assembly with a channel at nominal dimensions. This perturbation yielded a small reactivity effect of [] due to channel bulge.

Monte Carlo Calculation Uncertainty: The calculation uncertainty (standard deviation) for a single calculation (typically <0.0003) with a one-sided tolerance factor of $K = 1.7$ for 3000 neutron generations.

2

Uncertainty Introduced by Depletion Calculations

Critical experiment data are generally not available for spent fuel and; accordingly, some judgment must be used to assess uncertainties introduced by the depletion calculations. CASMO-4 and the 70 group cross section library used for these analyses has been used extensively to generate bundle average cross sections for core follow calculations and reload fuel design in both BWRs and PWRs. Any significant error in those depletion calculations would be detectable either by in-core instrumentation measurements of core power distributions or cycle energy output or both. Significant deviations between the predicted and actual fuel cycle lengths and core power distributions using CASMO-4 generated cross sections are not observed.

For the purpose of assessing the effects of uncertainties introduced by depletion calculations, it is useful to estimate the magnitude of depletion uncertainties in k_{∞} and compare this uncertainty with margins inherent in the present calculation. Reference 23 suggests a reactivity uncertainty equivalent to 5 percent of the reactivity decrement to the burnup of interest. For this analysis, in the absence of burnable absorbers, the reactivity decrement is [] Δk . The resulting burnup uncertainty would be [] Δk . For the limiting GNF 2 bundle at [] GWD/MTU, the uncertainty introduced by depletion is conservatively rounded up to [] in Δk and is included in Table 5-4.

2
3
3
2

Self-Shielding of Discrete Absorber Particle Size

The discrete absorber particle self-shielding bias accounts for the fact that Boraflex is made from discrete boron carbide particles and thus is not a homogeneous distribution of absorber particles. The effect of discrete particle self shielding was based on a typical particle distribution size for boron carbide used in Boraflex. The analysis indicated that an equivalent homogenous density of []% of the nominal B-10 density would yield a reactivity effect equivalent to an absorber panel containing discrete absorber particles^[25].

BADGER Measurement Bias

Review of the panel local dissolution effects from the Monte-Carlo analysis described in Section 4-2 indicated that each of the [] randomly generated panels included [] inches of shrinkage. As a conservative bound, approximately []" of total gap (or [] – 1/3rd inch cracks) corresponding to the maximum of 4.1% shrinkage (5.82") less 3.35" could be manifested as undetected cracks or local dissolution. For this bias, it was assumed that each panel contained [] cracks spaced axially on []" centers along the full length of the Boraflex panel. This is conservative in that gaps occur more or less in a random pattern which results in a lower reactivity effect. The reactivity effect of possible undetected cracks being observed as local dissolution is [] as shown in Table 4-1. The reactivity effect is listed in Table 4-1 and is added directly to the reference eigenvalue as listed in Table 5-4.

3
2
2

Leakage

The reactivity effect due to neutron leakage was analyzed by replacing the reflected boundary condition of the reference model 2-D KENO V.a with a water albedo in the z-direction. The net reactivity effect (credit) is [].

5.3.4 Space Between Modules

The reference CASMO calculations assume an infinitely repeating array of storage cells in the x and y directions as shown in Figure 2-4. In the Peach Bottom Unit 2 pool the individual storage cells are interconnected to form rack modules. One module typically consists of an array of 19 x 20 cells. A KENO V.a model was developed to determine reactivity effect of gaps at the module-to-module interface. Effectively, this model is an infinite array of 20 x 20 modules (modified in length for assembly drop analysis) each separated by 1.15 inch water gap in all directions. The result of this calculation indicates a net decrease in k_{eff} .

5.3.5 Summary of Reactivity Calculations

Table 5-4 contains a summary of the criticality analyses results for the Peach Bottom Unit 2 spent fuel racks. The nominal reference case k_{eff} for the GNF 2 fuel at [] w/o containing gadolinia rods is []. The results of tolerances and uncertainties when combined in a root-mean-square sense are []. At a 95% probability with a 95% confidence level the maximum k_{eff} of the Peach Bottom Unit 2 fuel racks loaded with GNF 2 fuel including all bias, tolerances and uncertainties is []. **The difference between this value and the $k_{\text{eff}} \leq 0.95$ design limit represents margin that is available to accommodate new fuel designs and to offset the effects of a fuel assembly misload. The resulting margin is [] for GNF 2 fuel up to [] w/o U^{235} with gadolinia.** The reactivity increase due to neutron spectral softening as caused by reduced Boraflex thickness, has been determined and included in the 95/95 maximum k_{eff} .

3
2

5.3.6 Abnormal/Accident Conditions

The following abnormal/accident conditions have been evaluated in order to determine the corresponding effects on fuel pool criticality:

- Fuel Assembly Drop
- Rack Lateral Movements

- Fuel Assembly Alongside Rack
- Moderator Density and Temperature Variations

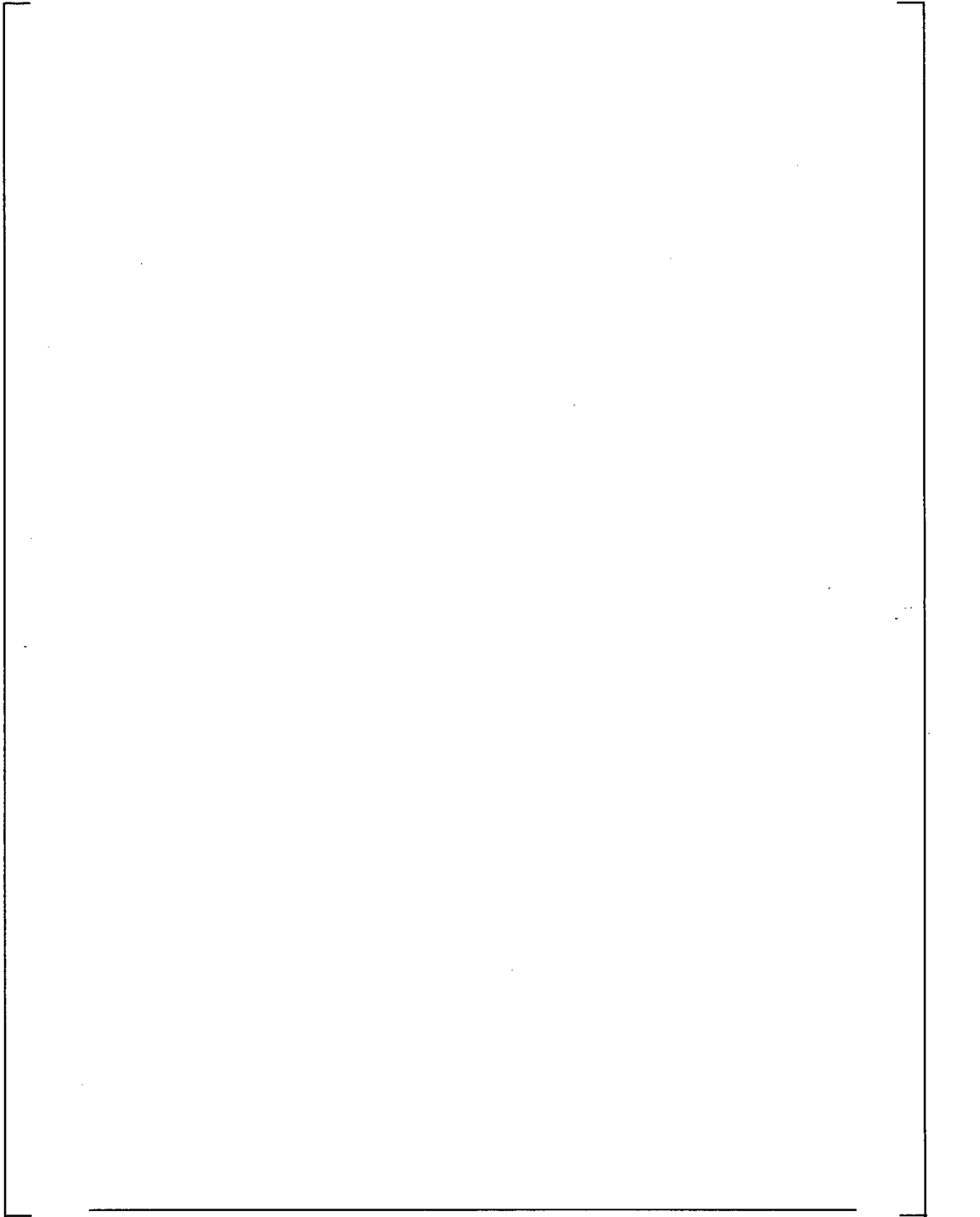
The drop of a fuel assembly with the assembly coming to rest in a horizontal position on top of the fuel and rack module has been evaluated. The resulting change in reactivity is slightly negative, however within the statistical uncertainty of the calculation (1σ) it is negligible.

Rack lateral motion can be postulated to occur during a seismic event. The racks have been analyzed at the minimum module-to-module spacing. Since all peripheral cell walls contain Boraflex, racks in contact would have 2 panels of Boraflex between adjacent fuel bundles. Therefore, the limiting condition is the reference infinite array and there is no further increase in reactivity due to rack lateral movement during a postulated seismic event. Analysis of a 1.15-inch gap between modules resulted in a lower k_{eff} relative to the infinite array.

The inadvertent positioning or the drop of a fuel assembly along side of a rack module between the module and the pool wall has been evaluated. The maximum increase in reactivity due to a dropped bundle is [] and is well within the sub-critical margin to the $k_{\text{eff}} \leq 0.95$ limit for accident conditions as specified by ANSI/ANS-57.2-1983. | 2

The effect of variations in moderator density and temperature on the reactivity of the Peach Bottom Unit 2 spent fuel storage racks have been analyzed. Loss of pool cooling has been postulated and analyzed at []°F and []°F and results in a lower k_{eff} relative to the reference case at maximum water density. Therefore, it is concluded that under worst-case accident conditions, the effective multiplication factor remains less than the $k_{\text{eff}} \leq 0.95$ limit, which applies to accident conditions. | 2

Table 5-4
Summary of Criticality Calculation Results
(10x10 Fuel)



6.0 Conclusions

The Peach Bottom Unit 2 spent fuel racks have been analyzed GNF 2 fuel with uniform initial enrichments of up to [] w/o U^{235} at a stack density of [] percent theoretical density. Maximum reactivity bundles with gadolinia for this fuel type have been specified requiring a minimum number of burnable poison rods per assembly and a minimum Gd_2O_3 loading per rod. Analyses have demonstrated that the maximum k_{eff} of the Peach Bottom Unit 2 spent fuel racks is less than 0.95 when loaded with maximum reactivity bundles of the GNF 2 fuel design and accounting for projected Boraflex degradation through May 1, 2010. The analyses contained herein are subject to the restriction that discharged fuel is placed in a B.5.b configuration in Modules 3, 4, 5 and 12 as described in Section 3.1 and as illustrated in Figure 3.2. | 2

The maximum k_{eff} of the Peach Bottom Unit 2 spent fuel racks will not exceed the 0.95 limit when loaded with GNF 2 fuel with a maximum bundle planer enrichment of [] w/o U^{235} (at [] percent theoretical density) with a minimum of [] gadolinia rods per fuel assembly each containing a minimum loading of [] w/o Gd_2O_3 .

For the most reactive loading ([] w/o U^{235} with [] gadolinia rods per fuel assembly) the margin to the $k_{eff} \leq 0.95$ design limit is []. When the worst case accident is imposed upon these conditions, k_{eff} remains below the accident condition regulatory limit of ≤ 0.95 . In all cases analyzed, conservative projections of Boraflex degradation through to May 1, 2010 were assumed. | 2

In order to insure that the projections of Boraflex degradation do not exceed [] (conservatively bounding), RACKLIFE projections should be verified with BADGER measurements. | 1 | 2 | 3

Since 1996, BADGER testing has been conducted in the spent fuel pools of each unit at Peach Bottom once every four years. Comparison of BADGER measurements with RACKLIFE predictions has shown the RACKLIFE predictions to be conservative. Accordingly, it is recommended that Exelon continue this practice. | 1

7.0 References

1. "An Assessment of Boraflex Performance in Spent-Nuclear-Fuel Storage Racks," Northeast Technology Corp. for the Electric Power Research Institute, NP-6159; December 1988.
2. "Boraflex Test Results and Evaluation", EPRI/TR-101986, prepared by Northeast Technology Corp. for the Electric Power Research Institute; February 1993.
3. "BADGER, a Probe for Non-destructive Testing of Residual Boron-10 Absorber Density in Spent-fuel Storage Racks: Development and Demonstration", EPRI TR-107335. Electric Power Research Institute: Palo Alto, CA; October 1997.
4. "The Boraflex Rack Life Extension Computer Code -- RACKLIFE: Theory and Numerics." EPRI TR-107333. Electric Power Research Institute: Palo Alto, CA; September 1997.
5. "The Boraflex Rack Life Extension Computer Code -- RACKLIFE: Verification and Validation." EPRI TR-109926. Electric Power Research Institute: Palo Alto, CA; March 1999.
6. "BADGER Demonstration at Peach Bottom Atomic Power Station Unit 2," NET-092-05, Rev. 0., Northeast Technology Corp. for the Electric Power Research Institute; August 1996.
7. "BADGER Test Campaign at Peach Bottom Unit 2", NET-192-01, Rev. 0., Northeast Technology Corp.: Kingston, NY; 22 May 2002.
8. " BADGER Test Campaign at Peach Bottom Unit 2", NET-264-01, Rev. 0., Northeast Technology Corp.: Kingston, NY; 21 June 2006.
9. "BADGER Test Campaign at Peach Bottom Unit 3", NET-174-01, Rev. 0, Northeast Technology Corp.: Kingston, NY; 9 July 2001.
10. "BADGER Test Campaign at Peach Bottom Unit 3", NET-247-01, Rev. 0, Northeast Technology Corp.: Kingston, NY; 6 August 2005.

NET-264-02 NP
Non-Proprietary Information Submitted in
Accordance with 10 CFR 2.390

11. "GNF2 Spent Fuel Rack Criticality Analysis for Peach Bottom Atomic Power Station Units 2 and 3," 000-0035-7327-SFR, Rev. 0; Global Nuclear Fuel; June 2005.
12. Orechwa, Y and Golla, J., "Safety Evaluation by the Office of Nuclear Reactor Regulation Related to Amendment No. 227 to Facility Operating License No. DPR-26 Entergy Nuclear Operations Inc., Indian Point Nuclear Generating Unit No. 2 Docket No. 50 - 247," 5/29/2002.
13. Email from J. Holley [Exelon] to M. Harris [NETCO] dated 12 July 2006.
14. "SCALE-PC: Modular Code System for Performing Criticality Safety Analyses for Licensing Evaluation, Version 5.0", Parts 1 through 3, RSIC Computer Code Collection CCC-725. Oak Ridge National Laboratory: Oak Ridge, Tennessee; May 2004.
15. Rhodes, Joel and Malte Edenius. "CASMO-4: A Fuel Assembly Burnup Program -- User's Manual", Version 2.05, Rev. 3. SSP-01/400. Studsvik of America: Newton, Massachusetts; July 2003.
16. Baldwin, M. N., G. S. Hoovler, R. L. Eng, and F. G. Welfare. "Critical Experiments Supporting Close Proximity Water Storage of Power Reactor Fuel," BAW-1484-7. Babcock & Wilcox: Lynchburg, Virginia; July 1979.
17. Mancioppi, S., and G. F. Gualdrini. "Standard Problem Exercise on Criticality Codes for Spent LWR Fuel Transport Containers," CNEN-RT/FI(81)25. Comitato Nazionale Energia Nucleare: Rome; October 1981. Alternately, OECD Nuclear Energy Agency, Committee on the Safety of Nuclear Installations, CSNI-71; 1982.
18. Bierman, S. R., E. D. Clayton, and B. M. Durst. "Critical Separation Between Subcritical Clusters of 2.35 Wt% ²³⁵U Enriched UO₂ Rods in Water with Fixed Neutron Poisons", PNL-2438. Battelle Pacific Northwest Laboratories: Richland, Washington; October 1977.
19. Bierman, S. R., E. D. Clayton, and B. M. Durst. "Critical Separation Between Subcritical Clusters of 2.35 Wt% ²³⁵U Enriched UO₂ Rods in Water with Fixed

NET-264-02 NP
Non-Proprietary Information Submitted in
Accordance with 10 CFR 2.390

Neutron Poisons", NUREG/CR-0073 RC. Battelle Pacific Northwest Laboratories: Richland, Washington; May 1978.

20. "Benchmarking of Computer Codes for Calculating the Reactivity State of Spent Fuel Storage Racks, Storage Casks and Transportation Casks," NET 901-02-05, Rev. 0, Northeast Technology Corp., Kingston, NY; 29 October 2004.
21. Jordan, W. C. "SCALE Cross Section Libraries", NUREG/CR-0200 Revision 7, Volume 3, Section M4, Oak Ridge National Laboratory: Oak Ridge, Tennessee; Draft May 2004.
22. Natrella, Mary Gibbons, Experimental Statistics, National Bureau of Standards Handbook 91; 1 August 1963.
23. Memorandum from L. Kopp, SRE, to Timothy Collins, Chief, Reactors System Branch, Division of Systems Safety and Analysis, "Guidance on the Regulatory Requirements for Criticality Analysis of Fuel Storage at Light Water Reactor Power Plants", August 19, 1998.
24. Broadhead, B., "Feasibility Assessment of Burnup Credit in the Criticality Analysis of Shipping Casks with Boiling Water Reactor Spent Fuel"; ORNL, Nuclear Technology, 110, 1-20; April 1995.
25. Doub, W.B., "Particle Self-Shielding in Plates Loaded with Spherical Poison Particles," Part B of Section 4.2, Naval Reactors Physics Handbook, Volume 1: Selected Basic Techniques, Naval Reactors, Division of Reactor Development, United States Atomic Energy Commission: Washington, D.C.; 1964.

Appendix A

**NET-264-02 NP
Non-Proprietary Information Submitted in
Accordance with 10 CFR 2.390**

**Appendix A
NET-901-02-05, Rev 3,
“Benchmarking of Computer Codes for
Calculating the Reactivity State of
Spent Fuel Storage Racks, Storage Casks and
Transportation Casks”**

**Benchmarking of Computer Codes
for
Calculating the Reactivity State
of
Spent Fuel Storage Racks, Storage Casks and Transportation
Casks**

Northeast Technology Corp.

108 North Front Street
Third Floor
UPO Box 4178
Kingston, New York
12402

Review/Approval Record

Rev.	Date	Prepared by:	Reviewed/Approved by:	Approved (QA) by:
3	2/6/09	<i>Matthew C. Harris</i>	<i>[Signature]</i>	<i>L.P. Mariani</i>

Note: New Revision signature sheet initiated due to classification of Revision 3 of NET-901-02-05 as a NETCO Proprietary Document.

Table of Contents

Section	Page
1.0 INTRODUCTION	1
2.0 BENCHMARKING - STANDARD PROBLEMS AND CONFIGURATION CONTROL	3
2.1 SCALE-5 and MCNP5 Configuration Control.....	3
2.2 Sample Problems	3
2.3 CASMO-4 Configuration Control.....	4
3.0 BENCHMARK MODELING OF LWR CRITICAL EXPERIMENTS	5
3.1 Benchmarking of SCALE-5 and MCNP5.....	5
3.2 Benchmarking of CASMO-4.....	12
4.0 CONCLUSIONS	14
5.0 REFERENCES	15

Report No. 901-02-05 NP, Rev 3
Non-Proprietary Information Submitted in
Accordance with 10 CFR 2.390

List of Tables

Table	Page
Table 3-1: B&W and PNL Critical Experiment Design Parameters.....	8
Table 3-2: KENO V.a and MCNP5 Critical Experiment Results.....	9
Table 3-3: B&W Critical Experiments as CASMO Infinite Arrays - Results	13

List of Figures

Figure	Page
Figure 3-1: Variation of Bias ($k_{eff} - 1$) with Moderator-to-Fuel Ratio	10
Figure 3-2: Variation of Bias ($k_{eff} - 1$) with Absorber Strength	11

1.0 INTRODUCTION

This report documents the results of benchmark calculations of three computer codes used to compute the reactivity state of nuclear fuel assemblies in close-packed arrays. Such close-packed arrays include high density spent fuel storage racks, dry storage casks and casks for transporting nuclear fuel. The three computer codes, which were benchmarked and validated are:

- KENO V.a, which is a module of SCALE 5^[1]
- MCNP5^[2]
- CASMO-4^[3]

Earlier versions of KENO and CASMO have been previously benchmarked and validated by NETCO.^[4,5] Most notably, the present version, which also includes MCNP, incorporates the results of fifty-two critical experiments whereas earlier versions incorporated thirteen critical experiments.

To benchmark and validate the codes for spent fuel racks and cask evaluations, KENO and MCNP were used to simulate a series of critical experiments. The calculated eigenvalues (k_{eff}) were then compared with the critical condition ($k_{\text{eff}} = 1.0$) to determine the bias inherent in the calculated values. For the KENO V.a calculation, the 238 energy group ENDF/B-V cross-section library was used. For the MCNP5 calculations, the continuous energy cross-section library based on ENDF/B-VI was used.

After determining the inherent biases associated with KENO V.a and MCNP5, both KENO V.a and CASMO-4 (with its own 70 energy group cross-section library) were used to model central arrays of select critical experiments. It is noted that CASMO-4 models an infinitely repeating array of fuel assemblies and is generally used to generate cross-sections for core simulator models. As such, it does not lend itself directly to finite arrays of fuel racks surrounded by a reflector, as is the case in the critical experiments considered. Accordingly, the central fuel arrays of five critical experiments were modeled as infinite arrays with both KENO V.a and CASMO-4. A comparison of the

KENO V.a and CASMO-4 eigenvalues provides a means to determine the CASMO-4 bias.

For the purposes of benchmarking, fifty-two critical experiments from the International Handbook of Evaluated Criticality Safety Benchmark Experiments^[6] were selected because they closely represent typical fuel/rack geometries with neutron absorber panels. The resulting models encompass the range of absorber strengths, moderator-to-fuel ratios and fuel rod geometries representative of most fuel storage rack and fuel cask configurations used today.

All work completed for the benchmarking calculations was carried out under NETCO's Quality Assurance Program^[7]. The methods employed have been patterned to comply with industry accepted standards^[8,9,10] and with accepted industry criticality references^[11,12, 13, 14, 15].

2.0 BENCHMARKING - STANDARD PROBLEMS AND CONFIGURATION CONTROL

2.1 SCALE-5 and MCNP5 Configuration Control

The binary executable codes and associated batch files were provided by RSICC on CD-ROM for use under the Windows operating system. In this form, the programs can not be altered or modified. In addition to the binary executable codes, there are several supporting files which contain cross-section sets, etc. Prior to executing either code sequence, the user will verify the file names, creation dates, and sizes to insure that they have not been changed.

2.2 Sample Problems

A suite of input files with their corresponding output files were provided with each code. These were executed on NETCO's host computer via batch files provided by RSICC and the resulting output files compared to those provided by RSICC on CD-ROM. Except for the date and time of execution stamps, the respective output files were identical. Each code uses a pseudo-random number generator that is initiated with a default seed value. Since the default value was used in each case, the sequences of random numbers were the same, leading to identical calculations. This verifies that the as-received versions of both codes are identical to the versions documented in the User's Manuals^[1,2].

Examination of the sample input decks shows that the run modules in batch files exercise all of the code options used by this benchmarking exercise. Before and after each subsequent use of each code, one set of sample input modules are executed and the output files compared to the sample output files to verify that no system degradation has occurred.

2.3 CASMO-4 Configuration Control

The version of CASMO-4 used for these analyses was developed for a RISCC workstation. Version 2.05 of CASMO-4 was used for this benchmarking work and subsequent users of CASMO-4 for NETCO will verify that Version 2.05 is being used. CASMO-4 and all versions are controlled by Studsvik of America under their Quality Assurance Program^[16]. If a different version of CASMO-4 is used by NETCO for any subsequent analyses, the CASMO-4 analyses in Section 3.2 shall be repeated with the version in use.

3.0 BENCHMARK MODELING OF LWR CRITICAL EXPERIMENTS

An index of input and output files for each experiment modeled is contained in the calculation notebook for this project and represents a permanent record of all hand and spreadsheet calculations performed during input preparation. All input parameters are fully traceable to the appropriate source documents.

3.1 BENCHMARKING OF SCALE-5 and MCNP5

The selected critical experiments include fifty-two (52) water moderated LWR fuel rod cores and close packed critical LWR fuel storage arrays. Of these, thirty-three were conducted at the Critical Mass Laboratory at the Pacific Northwest Laboratories (PNL). Twenty-one of the PNL critical experiments were either separated by water or stainless steel (i.e., had no neutron absorber plates). The remaining twelve PNL criticals had either borated stainless steel (of varying boron weight percents) or BORAL[®] absorber plates separating the fuel rod arrays.

The remaining nineteen critical experiments were performed at the Babcock & Wilcox (B&W) Lynchburg Research Center. These experiments involved 3X3 arrays of fuel rods with a uranium enrichment of [] w/o. The 3X3 arrays are surrounded by borated water. Four different loading configurations were used depending on the separation spacing (number of pin pitches) between fuel assemblies. Some experiments (CoreXI) merely used combinations of critical moderator height and soluble boron concentration.

In each MCNP5 model of the criticals, 6,000,000 neutrons in 3,000 generations were tracked. In each KENO model of the criticals, at least 6,000,000 neutrons in at least 3,000 generations were tracked. The output files were always checked to insure that the fission source distribution had converged. A summary of the distribution of k_{eff} over all generations is automatically plotted in the output files and shows them to be approximately normally distributed. Thus, normal one-sided tolerance limits with appropriate 95% probability / 95% confidence factors (95/95) can be used. The

Report No. 901-02-05 NP, Rev 3
Non-Proprietary Information Submitted in
Accordance with 10 CFR 2.390

enrichment). The coefficient of determination for bias versus absorber strength for the 238 Group ENDF/B-V library was an insignificant 4.4%, while for MCNP5, it was 10.8%. In all cases, the bias becomes less negative with increased absorber strength. These results are illustrated in Figures 3-1 and 3-2, respectively.

Table 3-1: B&W and PNL Critical Experiment Design Parameters

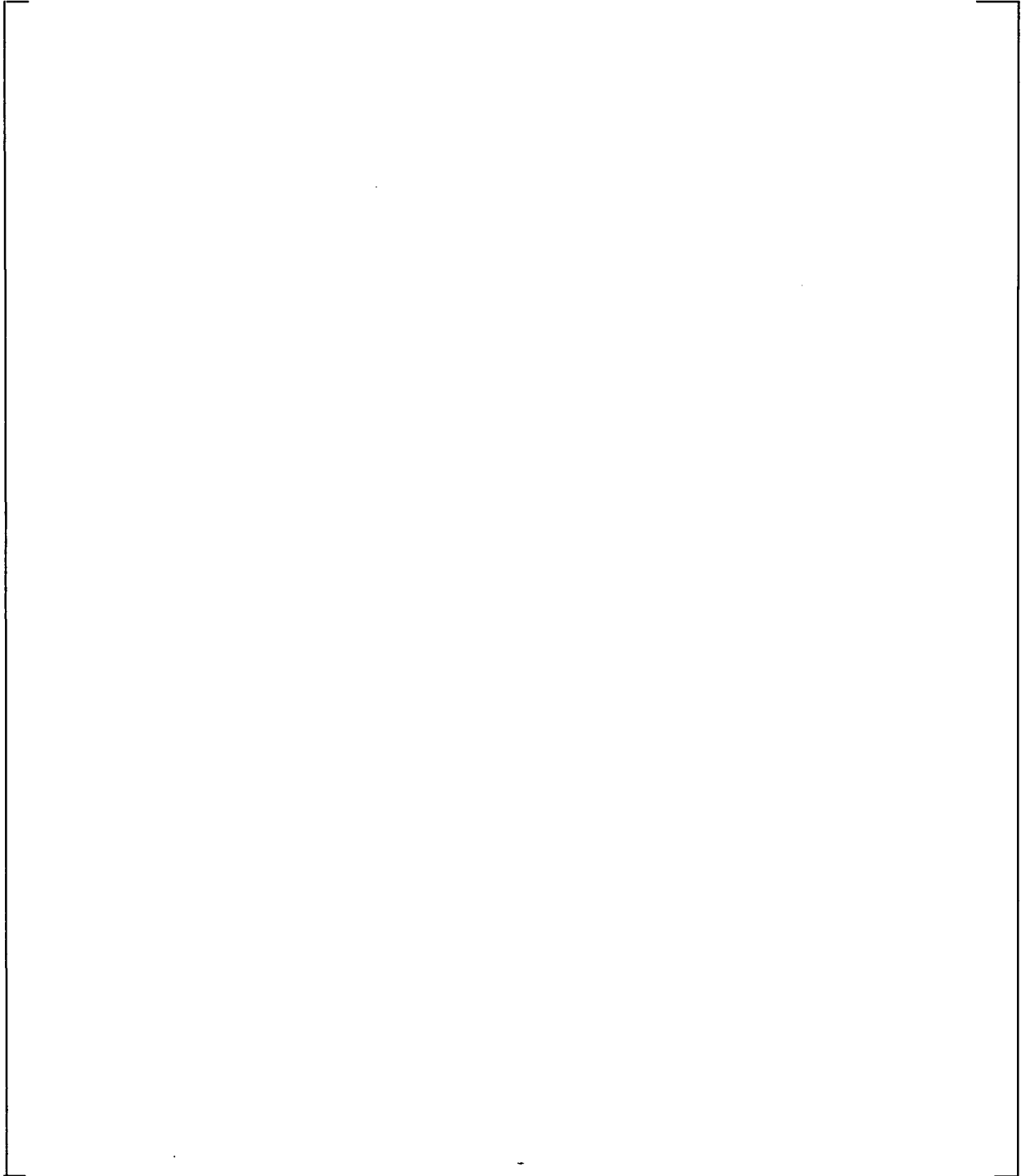
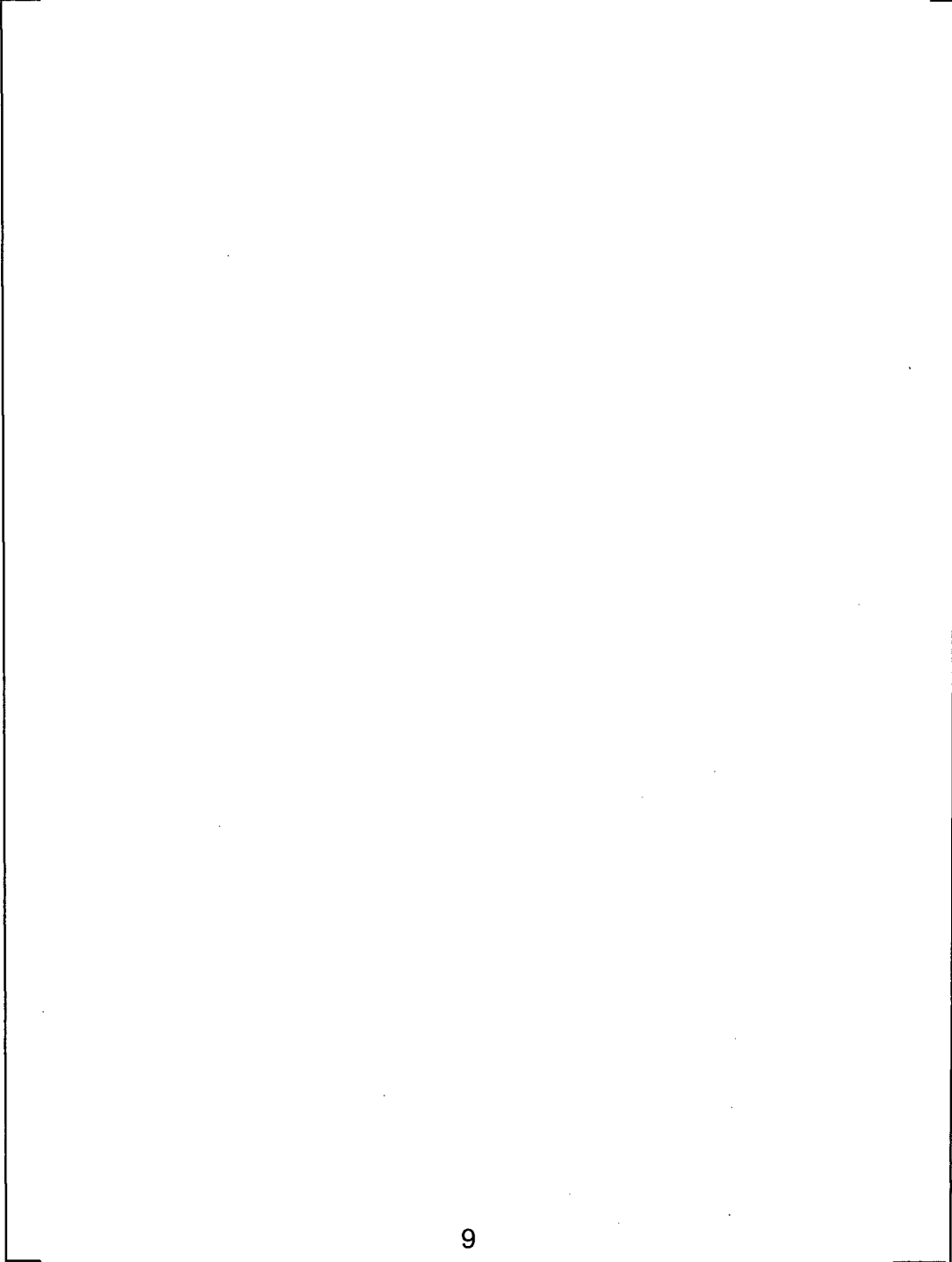


Table 3-2 KENO V.a and MCNP5 Critical Experiment Results



The table content is missing from the page, indicated by a large empty rectangular frame.

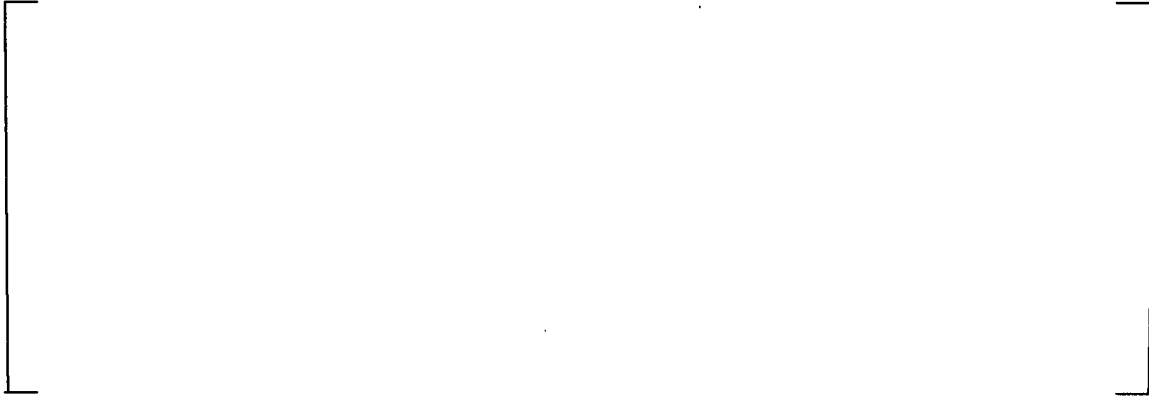


Figure 3-1: Variation of Bias ($k_{\text{eff}} - 1$) with Moderator-to-Fuel Ratio



Figure 3-2: Variation of Bias ($k_{\text{eff}} - 1$) with Absorber Strength

Table 3-3: B&W Critical Experiments as CASMO Infinite Arrays - Results

A large, empty rectangular box with a thin black border, positioned centrally on the page. It appears to be a placeholder for a table that is not present in this version of the document.

4.0 CONCLUSIONS

SCALE-5 and MCNP5 have been benchmarked by modeling nineteen (19) Babcock and Wilcox critical experiments and thirty-three (33) PNL critical experiments representative of fuel storage rack and fuel cask geometries. At a 95% probability / 95% confidence level, the computed bias uncertainties for SCALE-5 and MCNP5 are [] and [], respectively.

CASMO-4 has also been benchmarked by modeling nineteen (19) Babcock and Wilcox critical experiments as infinite arrays. Best estimates of the k_{∞} for the exact same geometry were calculated using SCALE-5 and applying the mean bias reported above. The CASMO-4 bias with respect to these values was calculated to be [

] (1 sigma). At a 95% probability / 95% confidence level, the bias uncertainty for CASMO-4 is []. The comparison of SCALE-5 and CASMO-4 serves to verify the results of each with respect to the other.

It is therefore concluded that these calculational methods have been adequately benchmarked and validated. They may be used individually or in combination for the criticality analysis of spent fuel storage racks, fuel casks and fuel casks in close proximity to fuel storage racks, provided the appropriate biases are applied.

The SCALE-5 bias with respect to these critical experiments was calculated to be []. The MCNP5 bias with respect to the critical experiments was calculated to be [].

5.0 REFERENCES

1. "SCALE-PC: Modular Code System for Performing Standardized Computer Analyses for Licensing Evaluation for Workstations and Personal Computers, Version 5," Volumes 0 through 3, RSIC Computer Code Collection CCC-725. Oak Ridge National Laboratory: Oak Ridge, Tennessee; Draft May 2004.
2. "MCNP – A General Monte Carlo N-Particle Transport Code, Version 5", Volumes 1 – 3, RSICC Computer Code Collection CCC-710, X-5 Monte Carlo Team, Los Alamos National Laboratory, Los Alamos, NM, April 24, 2003.
3. Ekberg, Kim, Bengt H. Forssen and Dave Knott. "CASMO-4: A Fuel Assembly Burnup Program - User's Manual," Version 1.10 STUDEVIK/SOA-95/1. Studsvik of America: Newton, Massachusetts; September 1995.
4. NETCO Report 901-02-03: "Benchmarking of the SCALE-PC Version 4.3 Criticality and Safety Analysis Sequence Using the KENO V.a Monte Carlo Code and of the Multigroup Two-Dimensional Transport Theory CASMO-4 Code", Northeast Technology Corporation: Kingston, New York; May 1995.
5. NETCO Report 901-02-04: "Benchmarking of the SCALE-PC Version 4.3 Criticality and Safety Analysis Sequence Using the KENO5A Monte Carlo code and of the Multigroup Two-Dimensional Transport Theory CASMO-4 Code", Northeast Technology Corporation: Kingston, New York; January 2000.
6. "International Handbook of Evaluated Criticality Safety Benchmark Experiments," NEA/NSC/DOE (95)03, September 2008 Edition. Nuclear Energy Agency, September 2008.
7. "Quality Assurance Manual, Rev. 1, Northeast Technology Corp: Kingston, NY; 10 August 2007.
8. "American National Standard for Nuclear Criticality Safety in Operations with Fissionable Materials Outside Reactors," ANSI/ANS-8.1-1983, Revision of ANSI/N 16.1-1975. American Nuclear Society: La Grange Park, Illinois; Approved 7 October 1983.

Report No. 901-02-05 NP, Rev 3
Non-Proprietary Information Submitted in
Accordance with 10 CFR 2.390

9. "Quality Assurance Requirements of Computer Software for Nuclear Facility Applications," Part 2.7 of "Quality Assurance Requirements for Nuclear Facility Applications," ASME NQA-2-1989, Revision of ANSI/ASME NQA-2-1986. American Society of Mechanical Engineers: New York; Issued 30 September 1989.
10. Natrella, Mary Gibbons. Experimental Statistics, National Bureau of Standards Handbook 91. U.S. Government Printing Office: Washington, D.C.; 1 Aug. 1963.
11. Cooney, B. F., T. R. Freeman, and M. H. Lipner. "Comparison of Experiments and Calculations for LWR Storage Geometries." Transactions of the American Nuclear Society: Vol. 39, pp. 531-532; November 1981.
12. Westfall, R. M., and J. R. Knight. "SCALE System Cross Section Validation with Shipping Cask Critical Experiments." Transactions of the American Nuclear Society: Vol. 33, pp. 368-370; 1979.
13. McCamis, R. H. "Validation of KENO V.a for Criticality Safety Calculations of Low-Enriched Uranium-235 Systems," AECL-10146-1. Atomic Energy of Canada Limited, Whiteshell Laboratories, Pinawa, Manitoba; February 1991.
14. Bierman, S. R., E. D. Clayton, and B. M. Durst. "Critical Separation Between Subcritical Clusters of 2.35 Wt% ²³⁵U Enriched UO₂ Rods in Water with Fixed Neutron Poisons," PNL-2438. Battelle Pacific Northwest Laboratories: Richland, Washington; October 1977.
15. Bierman, S. R., E. D. Clayton, and B. M. Durst. "Critical Separation Between Subcritical Clusters of 4.29 Wt% ²³⁵U Enriched UO₂ Rods in Water with Fixed Neutron Poisons," NUREG/CR-0073 RC. Battelle Pacific Northwest Laboratories: Richland, Washington; May 1978.
16. "Quality Assurance Program", SOA/REV 2. Studsvik of America: Newton, Massachusetts; Approved 16 August 1991.

Attachment 6

**Response to Request for Additional Information – Revision to
Technical Specification 4.3.1.1.a Concerning k-infinity, Revision 1
(Non-Proprietary Version)**

**Non-Proprietary Information Submitted
in Accordance with 10 CFR 2.390**

Attachment 6

Response to Request for Additional Information – Revision to
Technical Specification 4.3.1.1.a Concerning k-infinity

Revision 1

Page 1

Questions 16 – 25:

These questions have been deleted from this response. The criticality analysis applicable to Global Nuclear Fuel (GNF) has been deleted from this License Amendment Request (LAR). Therefore, Questions 16 through 25 are no longer applicable. Question 16 through 25 have not been answered because NET-264-02 P, evaluates the effects of Boraflex degradation and rack criticality in normal and off-normal conditions. The design basis lattice has been evaluated using the GNF TGBLA06A methodology to establish the new cold incore k_{∞} criteria of 1.318. Accordingly, Enclosures 5 and 6 (GNF documents) of the License Amendment Request (Letter from P. B. Cowan (Exelon Generation Company, LLC) to U. S. Nuclear Regulatory Commission, "License Amendment Request – Revision to Technical Specification 4.3.1.1.a Concerning k-infinity," dated June 25, 2008) are hereby withdrawn.

1. Question:

Proprietary and non-proprietary versions of technical report NET-264-02, "Criticality Analysis of the Peach Bottom Spent Fuel Racks for GNF-2 Fuel with Boraflex Panel degradation Projected to May 2012," are included in the LAR. NET-264-02 contains estimates of Boraflex degradation using testing conducted in accordance with EPRI (Electric Power Research Institute) TR-107335, "BADGER, a Probe for Non-destructive Testing of Residual Boron-10 Absorber Density in Spent-fuel Storage Racks: Development and Demonstration," and projections using EPRI TR-107333, "The Boraflex Rack Life Extension Computer Code - RACKLIFE: Theory and Numerics: and EPRI TR-109926, "The Boraflex Rack Life Extension Computer Code - RACKLIFE: Verification and Validation." NET-264-02 also uses what is described as, "... an advanced methodology..." and "...special algorithm..." in making the estimates. NET-264-02 asserts that, "The NRC has issued a Safety Evaluation Report accepting the methodology on a plant specific basis." However, the NRC safety evaluation cited was not issued to PBAPS. In addition, there is no description of the "...advanced methodology..." or "...special algorithm..." in the PBAPS SFP LAR or information that would allow the NRC to evaluate them on a plant-specific basis with regard to PBAPS. Please provide additional information that describes and justifies the use of the "advanced methodology" and "special algorithm" at PBAPS.

Response:

As discussed in Section 3.0 of the LAR, the methodology is based upon the approval of similar methodology for Indian Point. This methodology was cited as References 6 and 7 in the LAR. In the preparation of LARs that involve the application of methodologies, the standard and expected practice is to identify similar methodologies that have been accepted by NRC for other dockets, and apply these methodologies to the particular application. This practice provides a framework of predictability for Licensees in the preparation of LARs and reduces the time and cost in approving submittals. However, Exelon acknowledges NRC's concern that the referenced safety evaluation cited was not issued to Peach Bottom Atomic Power Station (PBAPS). Per NRC's request, Exelon is providing additional information to allow NRC to conclude that the NETCO methodology is acceptable for use at PBAPS.

**Non-Proprietary Information Submitted
in Accordance with 10 CFR 2.390**

Attachment 6

Response to Request for Additional Information – Revision to
Technical Specification 4.3.1.1.a Concerning k-infinity

Revision 1

Page 2

The "Advanced Methodology" and "Special Algorithm" refer to the Boraflex degradation feature sampling methodology developed by NETCO and documented in NET-264-03 P, Characterization of Boraflex Panel Degradation in the Peach Bottom Unit 2 Spent Fuel Pool Projected to May 2010".

2. Question:

The Boraflex degradation projected in NET-264-02 is based on an assumed future SFP loading and the associated gamma dose to the Boraflex panels. However, there is no information provided for the NRC to assess the reasonableness of this assumption. Please provide additional information that justifies the future SFP loading and associated gamma dose assumed in the LAR.

Response:

PBAPS is performing surveillances using RACKLIFE (as benchmarked with BADGER data) to ensure that pool average Boraflex degradation does not exceed [] and the peak panel degradation does not exceed []%. Compliance with these criteria will ensure operation within the constraints of the analysis.

3. Question:

An "average panel boron carbide loss" is projected in NET-264-02 and converted into an estimated uniform Boraflex panel thinning for the entire SFP. However, Figure 3-5 indicates that a large number of storage cells will have a projected individual "panel boron carbide loss" []. These storage cells are collocated, [] These localized circumstances are not addressed. Please provide information that addresses the localized effects of collocated storage cells and the localized k_{eff} values relative to the estimated uniform Boraflex panel thinning for the entire SFP.

Response:

The Reference case KENO V.a models are high fidelity [] arrays generated by sampling panels based on a distribution that reflects the projected boron carbide loss distribution in the PBAPS, Unit 2 spent fuel pool. These models are adjusted and verified to assure high loss panels are adequately sampled and preferentially placed adjacent to one another, such that the resulting boron carbide loss of the [] array bounds the worst rack modules in the spent fuel pool.

KENO V.a models of the limiting modules that contain arrays of cells with high loss panels [($> \text{---} \%$)] were also analyzed to verify that the reactivity effect of collocated panels did not exceed the reference case k_{∞} . Modules 7 (peripheral) and 12 (central) contain the largest arrays of high loss panels. These modules were modeled with 5x7 and 5x10 arrays of high loss panels [($\text{---} \%$)] and surrounded by rows of cells conservatively assumed to be at the highest loss that bounded adjacent cells (i.e., the highest loss for a block of cells was assumed for all

panels in that row). The models were infinite in the x, y and z directions using a periodic boundary condition in the x and y directions.

The KENO V.a calculations confirmed that the reference k_{∞} bounds the worst modules containing localized arrays of high loss panels. If an explicit model of the exact panel losses based on RACKLIFE projections to May 2010 were modeled, the reactivity effect would be even more negative due to conservatively neglecting lower loss panels that are present throughout the modules.

4. Question:

The Boraflex degradation projected in NET-264-02 is based on an end date of May 1, 2012. However, there is no proposed license condition that limits the licensee to that end date. Please provide a proposed license condition for the projected Boraflex degradation end date.

Response:

The analysis has been revised for an end date of May 2010. The date of the projection is merely a reference point in RACKLIFE. The critical values to monitor are the pool average boron carbide loss of [] for irradiated panels and peak panel loss of []. Should this boron carbide loss be approached, mitigation measures should be implemented.

Exelon hereby commits to resubmitting the analysis by December 31, 2009 incorporating a less reactive fuel bundle, and including an alternative loading pattern, if the analysis warrants. (See Attachment 2 for a discussion of the conservative, peak reactivity fuel bundle used in this LAR.) This new submittal will provide ample margin until further corrective actions can be developed and implemented that will resolve the Boraflex degradation issue. Further discussion of these corrective actions and the overall spent fuel management plan are in Attachment 2.

5. Question:

A two dimensional deterministic code, CASMO-4, is utilized in NET-264-02 to compute the reactivity effects due to degraded Boraflex. CASMO-4 is a proprietary computer code created by Studsvik. However, there is no generic Topical Report for CASMO-4, for either in-core analyses or in-rack analyses and the reference cited in NET-264-02 for CASMO-4 is not publicly available. While the NRC has approved the use of CASMO-4 as an approved methodology for in-core analysis methodologies at several licensees, this does not appear to be the case for PBAPS. There is no information provided for the staff to review regarding justifying the use of CASMO-4 specifically at PBAPS. Please provide information that justifies the use of CASMO-4 at PBAPS.

Response:

As similarly noted in Response Number 1, Exelon acknowledges that the absence of a generic Topical Report and safety evaluation specifically citing PBAPS has raised NRC's concerns regarding the use of CASMO-4 in this analysis. Per NRC's request, Exelon is providing

**Non-Proprietary Information Submitted
in Accordance with 10 CFR 2.390**

Attachment 6

Response to Request for Additional Information – Revision to
Technical Specification 4.3.1.1.a Concerning k-infinity

Revision 1

Page 4

additional information to allow NRC to conclude that the use of CASMO-4 is appropriate for this analysis.

NETCO has verified and validated CASMO-4 as documented in report NET-901-02-05 P, Revision 3, "Benchmarking of Computer Codes for Calculating the Reactivity State of Spent Fuel Storage Racks, Storage Casks and Transportation Casks" (Attachment A to NET-264-02 P). It should be noted that CASMO (due to its 2-D, infinitely reflected, rack model capabilities) has a limited number of critical experiments against which it can be validated. For the critical experiments evaluated, NETCO has determined the resulting CASMO-4 mean bias and standard deviation to be [] and [], respectively.

6. Question:

The [] in Table 5-4 is listed as [

[] Please provide justification that clarifies the source of the [] listed in Table 5.4.

Response:

The reference k_{∞} of [] (now [] based on []% thinning) in Table 5.4 of NET-264-02 P, is the KENO V.a value at a Reactivity Equivalent Fresh Fuel Enrichment and corrected for asymmetries in geometry modeling and cross-sections between CASMO-4 and KENO V.a. KENO V.a was executed by varying the U-235 enrichment to iteratively determine the REFFE that produced a k_{∞} of []. The REFFE that produced the same peak k_{∞} was [] w/o U-235.

CASMO-4 was used to determine the peak reactivity point during depletion. The peak k_{∞} (bias corrected) calculated by CASMO-4 was []. Geometry limitations in CASMO-4 prevent explicit modeling of the rack layout of the PBAPS, Unit 2 spent fuel rack cells. Therefore, a KENO V.a model that mirrored the CASMO geometry was created to verify the fidelity of the CASMO model. The difference between the CASMO-4 and KENO V.a models was negligible [()] and likely due to differences in cross sections confirming the fidelity of the CASMO model. An exact geometry model was subsequently created in KENO V.a to determine the reactivity bias between the exact geometry and the CASMO-4 geometry. The difference in reactivity between the exact geometry and the CASMO-4 geometry as calculated with KENO V.a was [] Δk . This reactivity bias was applied to the k_{∞} at peak reactivity. This results in a peak k_{∞} of [].

7. Question:

The information provided in the LAR and NET-264-02 is insufficient to evaluate the [] listed in Table 5-4. Please provide additional information to support the use of

**Non-Proprietary Information Submitted
in Accordance with 10 CFR 2.390**

Attachment 6

Response to Request for Additional Information – Revision to
Technical Specification 4.3.1.1.a Concerning k-infinity

Revision 1

Page 5

the [] listed in Table 5-4.

Response:

The base case KENO V.a was performed with infinite z boundary conditions. This case was compared with the similar case with water albedo boundary conditions in the upper and lower axial direction. The difference between these two values is [] Δk and represents the reactivity effect due to axial neutron leakage.

8. Question:

The information provided in the LAR and NET-264-02 is insufficient to evaluate the [] listed in Table 5-4. Please provide additional information to support the use of the [] listed in Table 5-4.

Response:

The reactivity effects of tolerances were determined by varying the parameter of interest to their upper and lower tolerance bounds and determining the worst case value in terms of reactivity relative to the nominal dimension. The tolerance values for each parameter as outlined in Section 5.3.3 of NET-264-02 P, are listed in the table below:

--

9. Question:

The [] listed in Table 5-4 of NET-264-02 appears to be the [

] Please provide additional information to support the selection of a 95/95 statistical tolerance value of 1.7 to the computed eigenvalues for KENO calculations as described on page 29 of NET-264-02.

**Non-Proprietary Information Submitted
in Accordance with 10 CFR 2.390**

Attachment 6

Response to Request for Additional Information – Revision to
Technical Specification 4.3.1.1.a Concerning k-infinity

Revision 1

Page 6

Response:

Fifty-two critical experiments have been analyzed with SCALE 5.0 and MCNP5 ver. 1.4. The results are summarized in NET-901-02-05, Revision 3, "Benchmarking of Computer Codes for Calculating the Reactivity State of Spent Fuel Storage Racks, Storage Casks and Transportation Casks" (Attachment A to NET-264-02 P).

Based upon 52 critical experiments, a one-sided (95/95) tolerance factor of 2.049 has been applied to the KENO V.a bias uncertainty.

10. Question:

NET-264-02 indicates the analysis is consistent with USNRC Regulatory Guide 1.13, "Spent Fuel Storage Facility Design Basis," and ANSI/ANS-57.2-1983, "Design Requirements for Light Water Reactor Spent Fuel Storage Facilities at Nuclear Power Plants." Regulatory Guide 1.13 does not address any criticality regulatory requirements such as Title 10 of the *Code of Federal Regulations* Part 50, Appendix A, General Design Criteria 62, "Prevention of criticality in fuel storage and handling," within its scope. Therefore, Regulatory Guide 1.13 should not be construed as endorsing the criticality requirements of ANSI/ANS-57.2-1983. Provide a justification for using the criticality requirements of ANSI/ANS-57.2-1983 as the methodology for the criticality analysis in the PBAPS SFP criticality analysis. In addition, not all of the items required by ANSI/ANS-57.2-1983 paragraph 6.4.2 appear to have been addressed (i.e. the requirements of 6.4.2.2.2 and 6.4.2.2.5 do not appear to be fully addressed). Therefore, please also provide additional information that addresses all items required by ANSI/ANS-57.2-1983 paragraph 6.4.2.

Response:

The original Regulatory Guide 1.13, issued in December 1975 did not endorse the requirements of ANSI/ANS-57.2-1983. However, Revision 2 to Regulatory Guide 1.13 in March 2007 (issued as Draft Regulatory Guide DG-1162 in October 2006) does endorse ANSI/ANS-57.2-1983, although the current status of this ANSI standard is indeterminate.

NET-264-02 P addresses the additional fuel rod tolerance uncertainties.

11. Question:

Appendix A of NET-264-02 documents benchmark calculations which determine computer code biases and uncertainties for KENO V.a, MCNP5 and CASMO-4. KENO V.a and MCNP5 are benchmarked to five criticality experiments which are common to other SFP criticality analyses and eight which are not. The vintage of the reference cited for the eight unfamiliar criticality experiments makes determining their validation difficult. Please provide additional information that supports the validation of the eight CSNI criticality experiments referred to in Section 4.0 of Appendix A of NET-264-02.

Response:

**Non-Proprietary Information Submitted
in Accordance with 10 CFR 2.390**

Attachment 6

Response to Request for Additional Information – Revision to
Technical Specification 4.3.1.1.a Concerning k-infinity

Revision 1

Page 7

As noted in the response to Question Number 9, Revision 3 of NET-901-02-05 has been provided as Appendix A to NET-264-02 P. Table 3-1 of Appendix A contains the list of critical experiments used in benchmarking SCALE-5, MCNP5 and CASMO-4.

12. Question:

[

] presented in Appendix A of NET-264-02. [

] presented in Appendix A of NET-264-02.

Response:

The results of the 52 critical benchmark experiments passed the tests for normality using the Anderson-Darling, Cramer-Von Mises and Kolmogorov-Smirnoff Tests for normality. Table A-7 of Experimental Statistics (Mary Gibbons Natrella, Experimental Statistics, National Bureau of Standards Handbook 91, August 1, 1963) contains one-sided tolerance factors for normal distributions for as few as 3 samples.

The 5 criticals employed in the CASMO-4 Benchmark were selected based on their being representative of typical fuel storage rack configurations similar to that at PBAPS.

13. Question:

Using the data provided in [] of Appendix A of NET-264-02 and the description of the treatment of the data, an NRC staff verification using a Microsoft Excel spreadsheet produces different results than those indicated [

] Please provide validation of the information indicated in [] of Appendix A of NET-264-02.

Response:

It was noted that while the values contained typographical errors, the bias reported was correct. The k_{∞} values were corrected.

14. Question:

Section 3.1 of Appendix A of NET-264-02 states the following: "For SCALE-5 the resulting mean bias for this library is -0.00782 ± 0.00361 . For MCNP5, using the continuous energy cross-section library based on ENDF/B-VI, the resulting variance weighted mean bias is -0.00574 ± 0.00509 ." Section 4.0 of Appendix A states the following: "At a 95% probability/95% confidence level, the computed bias for SCALE-5 and MCNP5 are -0.01381 and -0.01460 , respectively." The reason for the discrepancy between Section 3.1 and 4.0 of Appendix A of NET-264-02 is not apparent. Please provide additional information clarifying the apparent discrepancy.

Response:

The 95% probability/95% confidence level uncertainty is derived by multiplying the appropriate one-sided tolerance factor to the standard deviation in the bias. Since the uncertainties in the biases are statistical, they are treated in this manner and combined in the root-mean-square combination of tolerances and uncertainties in Table 5-4 of NET-264-02 P, for both CASMO-4 and KENO V.a.

15. Question:

Potential abnormal conditions for the PBAPS SFP are evaluated in NET-264-02. Page 39 of NET-264-02 concludes the following, "Therefore, it is concluded that under worst-case accident conditions, the effective multiplication factor remains less than the $k_{\text{eff}} \leq 0.98$ limit, which applies to accident conditions." However, the PBAPS Updated Final Safety Analysis Report (UFSAR), Section 10.3.3.1 states the following: "All arrangements of fuel in the spent fuel storage racks are maintained in a subcritical configuration having a $k_{\text{eff}} \leq 0.95$ for all conditions." The limit of $k_{\text{eff}} \leq 0.95$ is reiterated in Technical Specification 4.3.1.b, which also references Section 10.3 of the PBAPS UFSAR. Therefore, the analysis criteria presented in NET-264-02 does not appear to apply the current licensing basis for the PBAPS SFP. Please provide an explanation for the use of the $k_{\text{eff}} \leq 0.98$ criteria as opposed to the current licensing basis criteria of $k_{\text{eff}} \leq 0.95$ for all conditions. In addition, confirm that the proposed change will result in the current licensing basis being met for all conditions, including worst-case accident conditions. For example, adding the predicted k_{eff} value of [0.94881], reported in Section 5.3.5 of NET-264-02, with the Δk_{eff} value associated with a dropped bundle of [] (Section 5.3.6) results in a k_{eff} of []

Response:

The analysis has been performed for a nearer future date of May 2010 corresponding to a lesser amount of boron carbide loss. The rack average boron carbide loss at that time is []% with a maximum individual panel loss of []%. The equivalent thinning amount used in this analysis is []%, which yields a k_{ref} of [] as shown in Table 5.4. When all uncertainties and biases are considered, the calculated k_{eff} is []. Including the Δk_{eff} value associated with a dropped bundle of [], k_{eff} remains ≤ 0.95 for all conditions.